AIMS Mathematics, 11(1): 825–856.
DOI: 10.3934/math.2026036
Received: 13 October 2025
Revised: 17 December 2025
Accepted: 27 December 2025
Published: 12 January 2026

https://www.aimspress.com/journal/Math

Research article

Using a finite difference scheme together with neural networks analysis for propagation of the long waves equation

Thabet Abdeljawad[1,2,3], Kamal Shah[2,*], Israr Ahmad[4], Manel Hleili[5] and Maryam Salem Alatawi[5]

[1] Department of Fundamental Sciences, Faculty of Engineering and Architecture, Istanbul Gelisim University, 34310 Avcilar, Istanbul, Turkey

[2] Department of Mathematics and Sciences, Prince Sultan University, Riyadh 11586, Saudi Arabia

[3] Department of Medical Research, China Medical University, Taichung 40402, Taiwan

[4] Department of Mathematics, Government Post Graduate Jahanzeb College, Swat, KP, Pakistan

[5] Department of Mathematics, Faculty of Science, University of Tabuk, 71491 Tabuk, Saudi Arabia

* **Correspondence:** Email: kshah@psu.edu.sa; Tel: +923448054428.

Abstract: In this paper, we explored the Benjamin-Bona-Mahony-Burger (BBMB) equation in the context of the conformable fractional derivative. The major results are the existence, the uniqueness, and inaddition, the Ulam-Hyers (UH) stability of the solutions that are obtained, which guarantee the mathematical soundness of the proposed model. For the numerical study, the standard finite difference method (SFDM) and the non-standard finite difference method (NSFDM) were developed, and their performance was assessed through a comparison with the exact solution. The conclusions showed that NSFDM is more accurate and stable compared to SFDM. Additionally, a neural network (NN) scheme was used as a further validation tool, which was complemented by regression analysis and error distribution measures. The change of fractional order significantly affects the solution profiles, as shown by two or three-dimensional plots in numerical simulations. The fractional dynamics, therefore, play a crucial role in modifying wave propagation in more dimensions. The unique feature of this research is the joint use of conformable fractional calculus with NSFDM and neural computing for the BBMB equation, providing a new way for the treatment of nonlinear dispersive wave models.

Keywords: conformable derivative; BBMB equation; qualitative analysis; SFDM; NSFDM; neural network

Mathematics Subject Classification: 26A33, 34A08

1. Introduction

Fractional calculus (FC) is a straightforward generalization of classical calculus that differentiates and integrates not only integer orders but also non-integer orders. In fact, FC is the natural generalization. For this reason, researchers have been focusing on the development of the theoretical aspects as well as the investigations of practical applications of FC during the past three decades. Ahmad,et.al [1] have applied the tools of fractals fractional calculus to study Gumboro-Salmonella co-infection disease model. Ali,et.al [2] have investigated the BBMB equation by using iterative method. Podlubny [3] has produced the fundamental results of FC. Kilbas,et.al [4] have given the detailed analysis and results about the FC. FC has rapidly become a potential mathematical tool for science and technology, thanks to the great achievements in the field of science and technology, because of its power to model real-world processes with much more accuracy than the guiding integer-order methods. Hilfer [5] has introduced his famous fractional order derivative and integration called Ψ-Hilfer derivative. Magin [6] studied applications of FC in bioengineering. Authors [7] have studied Swift-Hohenberg equation by using iterative method.

The particular aspect of FC enables it to be efficient in simulating and computing complex dynamical systems. For instance, Tarasov [8] studied applications of FC in media and dynamics. The application of FC is diverse in disciplines such as electromagnetism, electrochemistry, fluid mechanics, signal processing, viscoelasticity, optics, and population dynamics [9]. Many contributions of FC are also available in the areas of turbulence, plasma physics, stochastic dynamical mechanisms, nonlinear control theory, and astrophysics, including controlled thermonuclear fusion [10]. Furthermore, fractional-order operators have been used in wave propagation, vehicular traffic flow, heat dissipation, and solid mechanics with great success.

Fractional partial differential equations (FPDEs) are indisputable tools in the analysis of dynamic systems and in the development of these nonlinear models [12]. FPDEs have been used to assess many real-world nonlinear phenomena and to bridge the gap between mathematical theory and physics. Bekir, et.al [11] have used first integral method in investigating solution of fractional differential equations. Also, Zhou [13] has introduced the basic theory of FC. Authors [14] have been studied the dynamics of nonlinear Burger equation by using the tools of FC. The methodologies that have been developed for the solutions of these problems mainly include the analytical and numerical methods, like the first integral method [15], the Elzaki transform decomposition method [16], the double Laplace transform method [17], the homotopy perturbation transform method [18], and the conformable Laplace transform approaches [19].

The Korteweg–de Vries (KdV) equation was introduced in 1895. The mentioned equations has very important applications to study the shallow water waves model. Authors [20] have solved the mentioned equation analytically in 1967. The rank extensions of KdV-type equations have arisen interest thanks to their use in plasma physics, nonlinear optics, and quantum mechanics. To deal with the drawbacks of the KdV model for small long waves, the Benjamin-Bona-Mahony (BBM) equation [21] was suggested in 1972. Researchers [22] have used linearized difference schemes to solve the mentioned problem which has been yielded more accurate results for shallow water and dispersive media. Later, the fractional BBM and BBMB equations were introduced to include non-locality, memory effects, and dissipative terms, thus making them more suitable in describing complex wave propagation. Hussain, et al. [23] have investigated the solotonic solutions of BBM equations.

Authors [24] have used numerical method to study the BBM equation.

The specified fractional BBMB equation of our study is given as follows:

$$\begin{cases} D_t^{\alpha} \mathsf{V}(\mathsf{x},\mathsf{t}) + \delta_1 \, \mathsf{V}_{\mathsf{x}}(\mathsf{x},\mathsf{t}) + \delta_2 \, \mathsf{V}^{\mathsf{m}} \mathsf{V}_{\mathsf{x}}(\mathsf{x},\mathsf{t}) - \delta_3 \, \mathsf{V}_{\mathsf{xxt}}(\mathsf{x},\mathsf{t}) - \delta_4 \mathsf{V}_{\mathsf{xx}}(\mathsf{x},\mathsf{t}) = 0, \\ \mathsf{V}(\mathsf{x},0) = f(x), \end{cases} \tag{1.1}$$

where δ_i for $i = 1, 2, 3, 4$ are constant parameters, and D_t^{α} represents a conformable fractional order derivative. Furthermore, one may note that $f(x)$ is continuous and bounded.

The BBM equation has been under study through different methods for the past few years, like finite difference methods [25], spline-based methods [26], Adomian decomposition [27], and homotopy analysis methods [28]. In our study, we explore the BBMB equation under conformable fractional derivative with the help of standard and non-standard finite difference numerical schemes. The main concern in the study is discussing the existence theory, stability analysis, and numerical simulations. Furthermore, we extend our analysis to NN to widen the scope of our study. The fractional operator taken in our analysis is more versatile in the prospect of modeling.

The remainder of this paper is organized as follows: In Section 2, we have presented the mathematical background, definitions, and properties of the conformable fractional derivative. In Section 3, the fractional-order BBMB equation and its theoretical background have been presented. In Section 4, we have addressed the UH stability of the proposed model. In Section 5, we have given details of the numerical schemes. In Section 6, the complete simulations have been given. In Section 7, the detailed information of the NN validation of the two specified numerical schemes has been discussed. Finally, in Section 8, we have given discussion and conclusion of results and future directions.

2. Preliminaries

In this section, we defines the basic ideas and results that are required for our work [29–31].

Definition 2.1. *For a function* $\mathbb{F} : [0, \infty) \to \mathbb{R}$, *the* α *order conformable fractional derivative* $\alpha \in (0, 1]$ *is defined as:*

$$D_t^{\alpha} \mathbb{F}(t) = \lim_{\epsilon \to 0} \left(\frac{\mathbb{F}(t + \epsilon \, t^{1-\alpha}) - \mathbb{F}(t)}{\epsilon} \right).$$

We say $\mathbb{F}$ *is* α*-differential if the conformable derivative of the function* $\mathbb{F}$ *of order* α *exists.*

Theorem 2.2. *Let* $\alpha \in (0, 1]$ *and* $\mathbb{F} : [0, \infty) \to \mathbb{R}$ *be differentiable. Then the conformable fractional derivative of* α *order is defined as:*

$$D_t^{\alpha} \mathbb{F}(t) = t^{1-\alpha} \frac{d\mathbb{F}}{dt}.$$

Definition 2.3. *Let* $\mathbb{F} : [0, \infty) \to \mathbb{R}$. *Then for all* $0 < t$, $\alpha \in (0, 1]$, *the conformable fractional integral of a function* $\mathbb{F}$ *is define as:*

$$\mathbb{I}_t^{\alpha} \mathbb{F}(t) = \int_0^t x^{\alpha - 1} \, \mathbb{F}(x) \, dx.$$

Theorem 2.4. $D_t^{\alpha} \mathbb{I}_t^{\alpha} \mathbb{F}(t) = \mathbb{F}(t)$, *for all* $0 < t$, *where* $\mathbb{F}$ *is continuous function on the domain of* $\mathbb{I}_t^{\alpha}$.

Theorem 2.5. *Let* $\mathbb{F} : (0, \infty) \to \mathbb{R}$ *be a differential and for all* $t > 0$, $\alpha \in (0, 1]$. *Then*

$$\mathbb{I}_t^{\alpha} \, D_t^{\alpha} \, \mathbb{F}(t) = \mathbb{F}(t) - \mathbb{F}(0).$$

3. Existence and uniqueness

The theoretical study of the specified problem is discussed in this section using Schauder and Banach theorems. For this purpose, we consider the Banach space, $\mathbb{X} = C([0,T]\times\mathbb{R})$, and the norm is defined as follows:

$$\|\mathsf{V}\| = \max_{x\in\mathbb{R},\, t\in \mathsf{J}} |\,\mathsf{V}(\mathsf{x},\mathsf{t})\,|, \text{ where } [0,T] = \mathsf{J}.$$

The general form of the problem (1.1) can be written as:

$$\begin{cases} D_t^{\alpha}\mathsf{V}(\mathsf{x},\mathsf{t}) = \psi(t,\mathsf{V}(\mathsf{x},\mathsf{t})) \\ \mathsf{V}(\mathsf{x},\mathsf{0}) = f(x). \end{cases} \tag{3.1}$$

Here, ψ is nonlinear and $f(x)$ is a continuous function.

Lemma 3.1. *The solution of general problem (3.1) is given as:*

$$\mathsf{V}(\mathsf{x},\mathsf{t}) = f(x) + \int_0^t s^{\alpha-1}\,\psi(s,\mathsf{V}(\mathsf{x},\mathsf{s}))\,ds.$$

For further work, one may write:

$$\mathcal{T}\,\mathsf{V}(\mathsf{x},\mathsf{t}) = f(x) + \int_0^t s^{\alpha-1}\,\psi(s,\mathsf{V}(\mathsf{x},\mathsf{s}))\,ds. \tag{3.2}$$

For further work the following assumptions are needed in our work:

(H_1) For $\mathsf{V}_1, \mathsf{V}_2 \in \mathbb{X}$, there exist a constant $L_\psi > 0$, such that

$$\|\psi(\mathsf{V}_1) - \psi(\mathsf{V}_2)\| \le L_\psi\,\|\mathsf{V}_1 - \mathsf{V}_2\|.$$

(H_2) For positive constants a_ψ and b_ψ, the growth condition for the non linear function ψ is given as:

$$\|\,\psi(\mathsf{V})\| \;=\; a_\psi + b_\psi\,\|\mathsf{V}\|.$$

Theorem 3.2. *Under the assumption* (H_1)*, the problem* (3.2) *has a unique solution if it holds* $L_\psi T^\alpha < \alpha$.

Proof. Considering, $\mathsf{V}_1, \mathsf{V}_2 \in \mathbb{X}$, we have

$$\begin{aligned}
\|\mathcal{T}\,\mathsf{V}_1 - \mathcal{T}\,\mathsf{V}_2\| &= \max_{x\in\mathbb{R},\, t\in\mathsf{J}} \left| \int_0^t s^{\alpha-1}\psi\left(s,\mathsf{V}_1(\mathsf{x},\mathsf{s})\right) ds - \int_0^t s^{\alpha-1}\psi\left(s,\mathsf{V}_2(\mathsf{x},\mathsf{s})\right) ds \right| \\
&\le \max_{x\in\mathbb{R},\, t\in\mathsf{J}} \int_0^t \left| s^{\alpha-1}\left(\psi\left(s,\mathsf{V}_1(\mathsf{x},\mathsf{s})\right) - \psi\left(s,\mathsf{V}_2(\mathsf{x},\mathsf{s})\right)\right)\right| ds \\
&\le \max_{x\in\mathbb{R},\, t\in\mathsf{J}} \left|\psi\left(s,\mathsf{V}_1(\mathsf{x},\mathsf{s})\right) - \psi\left(s,\mathsf{V}_2(\mathsf{x},\mathsf{s})\right)\right| \int_0^t s^{\alpha-1} ds \\
&\le L_\psi\,\|\mathsf{V}_1 - \mathsf{V}_2\|\,\frac{T^\alpha}{\alpha} \\
&\le \frac{L_\psi T^\alpha}{\alpha}\,\|\mathsf{V}_1 - \mathsf{V}_2\|.
\end{aligned}$$

Therefore, in-light of the Banach contraction principle, problem (3.2) possesses a unique solution. □

Theorem 3.3. *Under the assumptions* (H_1)-(H_2)*, problem* (3.1) *has at least one solution.*

Proof. We show that the operator $\mathcal{T} : \mathbb{X} \to \mathbb{X}$ satisfies the conditions of Schauder's fixed-point theorem.

Let $\mathtt{M} = \max_{x\in\mathbb{R}} |f(x)|$. Choose $\mathfrak{r} > 0$, such that

$$\mathtt{M} + \frac{T^\alpha}{\alpha}(a_\psi + b_\psi \mathfrak{r}) \leq \mathfrak{r},$$

and define the closed convex set

$$\mathbb{B} = \{\mathsf{V} \in \mathbb{X} : \|\mathsf{V}\| \leq \mathfrak{r}\}.$$

The proof is divided into verifying the two major hypotheses of Schauder's theorem.

(i) Continuity of $\mathcal{T}$: Let $\{\mathsf{V}_n\} \subset \mathbb{B}$ with $\mathsf{V}_n \to \mathsf{V}$ in $\mathbb{X}$. Using assumption (H_1),

$$\begin{aligned}
\|\mathcal{T}\mathsf{V}_n - \mathcal{T}\mathsf{V}\| &= \max_{x\in\mathbb{R},\, t\in\mathrm{J}} \left| \int_0^t s^{\alpha-1} \left[\psi(s, \mathsf{V}_n(x,s)) - \psi(s, \mathsf{V}(x,s))\right] ds \right| \\
&\leq \max_{x\in\mathbb{R},\, t\in\mathrm{J}} \int_0^t s^{\alpha-1} \left|\psi(s, \mathsf{V}_n(x,s)) - \psi(s, \mathsf{V}(x,s))\right| ds \\
&\leq L_\psi \|\mathsf{V}_n - \mathsf{V}\| \max_{t\in\mathrm{J}} \int_0^t s^{\alpha-1} ds \\
&= \frac{L_\psi T^\alpha}{\alpha} \|\mathsf{V}_n - \mathsf{V}\| \to 0 \quad \text{as } n \to \infty.
\end{aligned}$$

Hence, $\mathcal{T}$ is continuous on $\mathbb{B}$.

Compactness of $\mathcal{T}(\mathbb{B})$: We show that $\mathcal{T}(\mathbb{B})$ is relatively compact in $\mathbb{X}$ via the Arzelà–Ascoli theorem.

(ii) Uniform boundedness: For any $\mathsf{V} \in \mathbb{B}$, using (H_2),

$$\begin{aligned}
\|\mathcal{T}\mathsf{V}\| &= \max_{x\in\mathbb{R},\, t\in\mathrm{J}} \left| f(x) + \int_0^t s^{\alpha-1} \psi(s, \mathsf{V}(x,s)) ds \right| \\
&\leq \mathtt{M} + \max_{t\in\mathrm{J}} \int_0^t s^{\alpha-1} \left|\psi(s, \mathsf{V}(x,s))\right| ds \\
&\leq \mathtt{M} + \max_{t\in\mathrm{J}} \int_0^t s^{\alpha-1} \left(a_\psi + b_\psi \|\mathsf{V}\|\right) ds \\
&\leq \mathtt{M} + \frac{T^\alpha}{\alpha}(a_\psi + b_\psi \mathfrak{r}) \leq \mathfrak{r}.
\end{aligned}$$

Thus, $\mathcal{T}(\mathbb{B})$ is uniformly bounded.

(iii) Equicontinuity in t: Let $t_1, t_2 \in \mathrm{J}$ with $t_2 > t_1$ and $\mathsf{V} \in \mathbb{B}$. Then using assumption (H_2), we have

$$\begin{aligned}
|(\mathcal{T}\mathsf{V})(x,t_2) - (\mathcal{T}\mathsf{V})(x,t_1)| &= \left| \int_{t_1}^{t_2} s^{\alpha-1} \psi(s, \mathsf{V}(x,s)) ds \right| \\
&\leq \int_{t_1}^{t_2} s^{\alpha-1} \left|\psi(s, \mathsf{V}(x,s))\right| ds
\end{aligned}$$

$$\leq (a_\psi + b_\psi \mathfrak{r}) \int_{t_1}^{t_2} s^{\alpha-1} ds$$
$$= \left(\frac{a_\psi + b_\psi \mathfrak{r}}{\alpha} \right) (t_2^\alpha - t_1^\alpha).$$

As $t_2 \to t_1$, one may get $\|\mathcal{T}\,\mathsf{V}(\mathsf{x}, \mathsf{t}_1) - \mathcal{T}\,\mathsf{V}(\mathsf{x}, \mathsf{t}_2)\| \to 0$. The aforementioned steps show that $\mathcal{T}(\mathbb{B})$ is equi-continuous. By Arzelà–Ascoli, $\mathcal{T}(\mathbb{B})$ is relatively compact in $\mathbb{X}$. Hence, all conditions of Schauder's fixed-point theorem are satisfied. So the integral equation (3.2) has a fixed point. Consequently, problem (3.1) has at least one solution. □

4. Stability analysis

To be dependable for application to real situations, mathematical models have to be stable, as this ensures that even very small changes in the initial conditions or parameters will result in bounded and predictable solutions. The practical usefulness of a model may be limited by the provision of wildly divergent solutions without stability. Stability in dynamic systems also implies disturbance robustness, which is required to provide repeated behavior under a range of conditions and consistent long-term predictions [32].

Consider problem (3.1) as follows:

$$D_t^\alpha \mathsf{V}(\mathsf{x}, \mathsf{t}) = \psi(t, \mathsf{V}(\mathsf{x}, \mathsf{t})) + h(t). \tag{4.1}$$

Where $h(t)$ is a continuous function such that $h(t) \leq \theta$, for $\theta > 0$ and $t \in \mathrm{J}$. The solution of problem (4.1) is obtain as follows:

$$\mathsf{V}(\mathsf{x}, \mathsf{t}) = f(x) + \int_0^t s^{\alpha-1} \left(\psi(s, \mathsf{V}(\mathsf{x}, \mathsf{s})) + h(s) \right) ds$$
$$\mathsf{V}(\mathsf{x}, \mathsf{t}) = f(x) + \int_0^t s^{\alpha-1} \psi(s, \mathsf{V}(\mathsf{x}, \mathsf{s})) \, ds + \int_0^t s^{\alpha-1} h(s) \, ds$$

Using Eq (3.2), we have

$$\mathsf{V}(\mathsf{x}, \mathsf{t}) = \mathcal{T}\mathsf{V}(\mathsf{x}, \mathsf{t}) + \int_0^t s^{\alpha-1} h(s) \, ds$$
$$\|\mathsf{V}(\mathsf{x}, \mathsf{t}) - \mathcal{T}\mathsf{V}(\mathsf{x}, \mathsf{t})\| = \max_{x \in \mathbb{R},\, t \in \mathrm{J}} \left| \mathcal{T}\mathsf{V}(\mathsf{x}, \mathsf{t}) + \int_0^t s^{\alpha-1} h(s) \, ds - \mathcal{T}\mathsf{V}(\mathsf{x}, \mathsf{t}) \right|$$
$$\leq \max_{x \in \mathbb{R},\, t \in \mathrm{J}} \int_0^t |h(s)| \, s^{\alpha-1} \, ds$$
$$\leq \frac{T^\alpha}{\alpha} \theta.$$

Theorem 4.1. *The solution of problem (3.1) is UH and generalized UH stable provided that*

$$\frac{L_\psi T^\alpha}{\alpha} < 1.$$

Proof. Let $\mathsf{V}(x,t)$ be any solution of the inequality

$$\|\mathsf{V}(x,t) - \mathcal{T}\mathsf{V}(x,t)\| \leq \theta,$$

and let $\mathsf{V}^\star(x,t)$ be the unique fixed point of $\mathcal{T}$. Then

$$\begin{aligned}\|\mathsf{V}(x,t) - \mathsf{V}^\star(x,t)\| &= \|\mathsf{V}(x,t) - \mathcal{T}\mathsf{V}^\star(x,t)\| \\ &\leq \|\mathsf{V}(x,t) - \mathcal{T}\mathsf{V}(x,t)\| + \|\mathcal{T}\mathsf{V}(x,t) - \mathcal{T}\mathsf{V}^\star(x,t)\| \\ &\leq \theta + \frac{L_\psi T^\alpha}{\alpha}\|\mathsf{V}(x,t) - \mathsf{V}^\star(x,t)\|.\end{aligned}$$

Rearranging gives

$$\left(1 - \frac{L_\psi T^\alpha}{\alpha}\right)\|\mathsf{V}(x,t) - \mathsf{V}^\star(x,t)\| \leq \theta,$$

and hence

$$\|\mathsf{V}(x,t) - \mathsf{V}^\star(x,t)\| \leq \frac{\theta}{1 - \frac{L_\psi T^\alpha}{\alpha}} = \frac{\alpha\theta}{\alpha - L_\psi T^\alpha}.$$

Setting $C = \frac{\alpha}{\alpha - L_\psi T^\alpha} > 0$, we obtain

$$\|\mathsf{V}(x,t) - \mathsf{V}^\star(x,t)\| \leq C\,\theta.$$

Thus, the problem is UH stable.

For generalized UH stability, let $\zeta(\theta) = \theta$ (which is non-decreasing and $\zeta(0) = 0$). Then

$$\|\mathsf{V}(x,t) - \mathsf{V}^\star(x,t)\| \leq C\,\zeta(\theta),$$

which proves generalized UH stability. □

Before going to the next sections, we provide the following flowchart 1 for the readers.

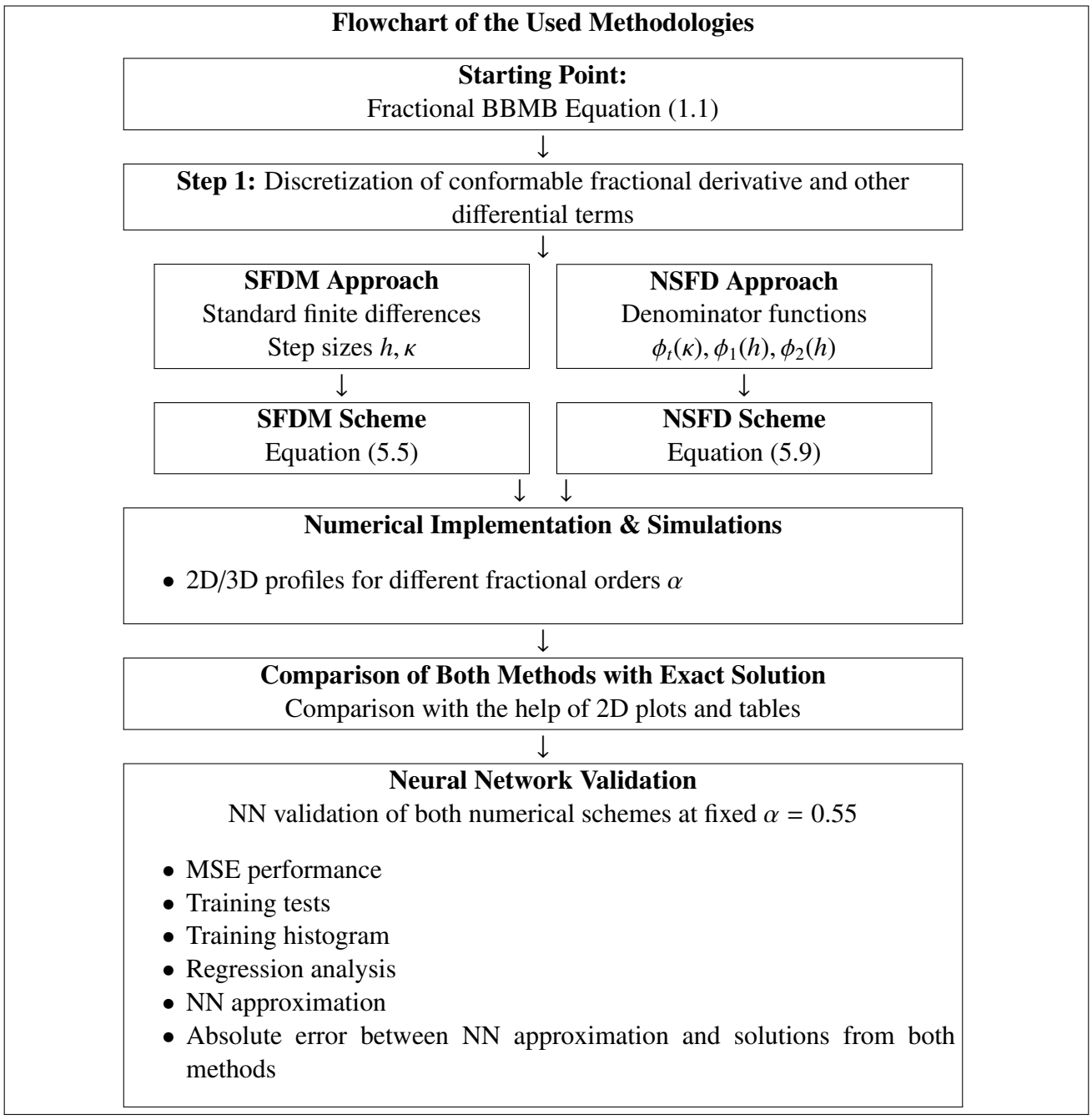

Figure 1. Flowchart of numerical schemes and validation procedures.

5. Numerical schemes of the proposed model

In the study of non-linear analysis, numerical solutions play a vital role because, most of the time in real world problems, it is difficult to find the closed form solutions [33]. Therefore, we consider the fractional BBMB equation under the conformable derivative to study the dynamics of the model in detail by utilizing the SFDM and NSFDM. The SFDM has standard discretization compared to the NSFDM, which has more liberty in the discretization process. The NSFDM not only guarantees the

trustworthiness but also demonstrates the importance of advanced discretization methods in improving the reliability and precision of fractional models, [34].

5.1. A standard finite difference scheme with a conformable derivative

We approximate the fractional term $D_t^{\alpha}\mathsf{V}(x,t)$ by the conformable finite difference scheme and discretize the spatial derivatives using standard central differences. Applying these discretizations to Eq (1.1) yields:

$$\begin{aligned}(n\kappa)^{1-\alpha}\left(\frac{\mathsf{V}_i^{n+1}-\mathsf{V}_i^n}{\kappa}\right)+\delta_1\left(\frac{\mathsf{V}_{i+1}^n-\mathsf{V}_i^n}{h}\right)+\delta_2(\mathsf{V}_i^n)^m\left(\frac{\mathsf{V}_{i+1}^n-\mathsf{V}_i^n}{h}\right)\\ -\delta_3\frac{1}{\kappa h^2}\Big(\mathsf{V}_{i+1}^{n+1}+\mathsf{V}_{i-1}^{n+1}-2\mathsf{V}_i^{n+1}+2\mathsf{V}_i^n-\mathsf{V}_{i+1}^n-\mathsf{V}_{i-1}^n\Big)\\ -\delta_4\left(\frac{\mathsf{V}_{i+1}^n-2\mathsf{V}_i^n+\mathsf{V}_{i-1}^n}{h^2}\right)=0.\end{aligned} \tag{5.1}$$

Multiplying with κ and simplifying the temporal fractional term, Eq (5.1) gives:

$$\begin{aligned}n^{1-\alpha}\kappa^{-\alpha}(\mathsf{V}_i^{n+1}-\mathsf{V}_i^n)-\frac{\delta_3}{h^2}(\mathsf{V}_{i+1}^{n+1}+\mathsf{V}_{i-1}^{n+1}-2\mathsf{V}_i^{n+1}+2\mathsf{V}_i^n-\mathsf{V}_{i+1}^n-\mathsf{V}_{i-1}^n)\\ =-\kappa\delta_1\left(\frac{\mathsf{V}_{i+1}^n-\mathsf{V}_i^n}{h}\right)-\kappa\delta_2(\mathsf{V}_i^n)^m\left(\frac{\mathsf{V}_{i+1}^n-\mathsf{V}_i^n}{h}\right)\\ +\kappa\delta_4\left(\frac{\mathsf{V}_{i+1}^n-2\mathsf{V}_i^n+\mathsf{V}_{i-1}^n}{h^2}\right).\end{aligned} \tag{5.2}$$

Collecting the unknown time-level $(n+1)$ terms on the left-hand side and the known time-level (n) terms on the right-hand side in Eq (5.2), we obtain:

$$\begin{aligned}&n^{1-\alpha}\kappa^{-\alpha}\mathsf{V}_i^{n+1}-\frac{\delta_3}{h^2}(\mathsf{V}_{i+1}^{n+1}+\mathsf{V}_{i-1}^{n+1}-2\mathsf{V}_i^{n+1})\\ &=n^{1-\alpha}\kappa^{-\alpha}\mathsf{V}_i^n-\frac{\delta_3}{h^2}(2\mathsf{V}_i^n-\mathsf{V}_{i+1}^n-\mathsf{V}_{i-1}^n)\\ &\quad-\frac{\kappa\delta_1}{h}(\mathsf{V}_{i+1}^n-\mathsf{V}_i^n)-\frac{\kappa\delta_2}{h}(\mathsf{V}_i^n)^m(\mathsf{V}_{i+1}^n-\mathsf{V}_i^n)+\frac{\kappa\delta_4}{h^2}(\mathsf{V}_{i+1}^n-2\mathsf{V}_i^n+\mathsf{V}_{i-1}^n).\end{aligned} \tag{5.3}$$

Keeping similar spatial discretization terms together, we rewrite Eq (5.3) as:

$$\begin{aligned}&\left(n^{1-\alpha}\kappa^{-\alpha}+\frac{2\delta_3}{h^2}\right)\mathsf{V}_i^{n+1}-\frac{\delta_3}{h^2}\mathsf{V}_{i+1}^{n+1}-\frac{\delta_3}{h^2}\mathsf{V}_{i-1}^{n+1}\\ &=\left(n^{1-\alpha}\kappa^{-\alpha}+\frac{2\delta_3}{h^2}-\frac{2\kappa\delta_4}{h^2}+\frac{\kappa\delta_1}{h}+\frac{\kappa\delta_2}{h}(\mathsf{V}_i^n)^m\right)\mathsf{V}_i^n\\ &\quad+\left(\frac{\kappa\delta_4}{h^2}-\frac{\delta_3}{h^2}-\frac{\kappa\delta_1}{h}-\frac{\kappa\delta_2}{h}(\mathsf{V}_i^n)^m\right)\mathsf{V}_{i+1}^n\\ &\quad+\left(\frac{\kappa\delta_4}{h^2}-\frac{\delta_3}{h^2}\right)\mathsf{V}_{i-1}^n.\end{aligned} \tag{5.4}$$

Finally, rearranging Eq (5.4) into a more compact form gives the generalized SFDM scheme for the BBMB equation (1.1):

$$\begin{aligned}
&\left(n^{1-\alpha}\,\kappa^{-\alpha}+\frac{2\delta_3}{\kappa h^2}\right)\mathsf{V}_i^{n+1}-\frac{\delta_3}{\kappa h^2}\mathsf{V}_{i+1}^{n+1}-\frac{\delta_3}{\kappa h^2}\mathsf{V}_{i-1}^{n+1}\\
&=-\left(\frac{\delta_3}{\kappa h^2}+\frac{\delta_1}{h}-\frac{\delta_4}{h^2}\right)\mathsf{V}_{i+1}^{n}+\left(\frac{2\delta_3}{\kappa h^2}+\frac{\delta_1}{h}-\frac{2\delta_4}{h^2}+n^{1-\alpha}\kappa^{-\alpha}\right)\mathsf{V}_i^{n}\\
&\quad+\left(\frac{\delta_4}{h^2}-\frac{\delta_3}{\kappa h^2}\right)\mathsf{V}_{i-1}^{n}+\frac{\delta_2}{h}(\mathsf{V}_i^{n})^{m}(\mathsf{V}_i^{n}-\mathsf{V}_{i+1}^{n}).
\end{aligned}\tag{5.5}$$

Equation (5.5) is the desired fully discrete SFDM scheme for the time-fractional BBMB equation (1.1) with a conformable derivative.

5.2. The non- standard finite difference method scheme with conformable derivatives

First, we approximate the fractional derivative using the conformable operator and replace the classical finite-difference denominators with appropriate denominator functions [35]:

$$\phi_t(\kappa),\qquad \phi_1(h),\qquad \phi_2(h),$$

where ϕ_1,ϕ_2 are used for the first and second spatial derivatives, and ϕ_t is a time denominator that accommodates the fractional time behavior. Applying these to Eq (1.1) gives:

$$\begin{aligned}
&(n\kappa)^{1-\alpha}\left(\frac{\mathsf{V}_i^{n+1}-\mathsf{V}_i^{n}}{\phi(\kappa)}\right)+\delta_1\left(\frac{\mathsf{V}_{i+1}^{n}-\mathsf{V}_i^{n}}{\phi_1(h)}\right)+\delta_2\,\mathsf{V}_{i+1}^{n}(\mathsf{V}_i^{n})^{m-1}\left(\frac{\mathsf{V}_{i+1}^{n}-\mathsf{V}_i^{n}}{\phi_1(h)}\right)\\
&-\delta_3\frac{1}{\phi(\kappa)(\phi_2(h))^2}(\mathsf{V}_{i+1}^{n+1}+\mathsf{V}_{i-1}^{n+1}-2\mathsf{V}_i^{n+1}+2\mathsf{V}_i^{n}-\mathsf{V}_{i+1}^{n}-\mathsf{V}_{i-1}^{n})\\
&-\delta_4\left(\frac{\mathsf{V}_{i+1}^{n}-2\mathsf{V}_i^{n}+\mathsf{V}_{i-1}^{n}}{(\phi_2(h))^2}\right)=0.
\end{aligned}\tag{5.6}$$

After expanding and collecting terms in Eq (5.6), we obtain:

$$\begin{aligned}
&\frac{(n\kappa)^{1-\alpha}}{\phi(\kappa)}\mathsf{V}_i^{n+1}-\frac{(n\kappa)^{1-\alpha}}{\phi(\kappa)}\mathsf{V}_i^{n}+\frac{\delta_1}{\phi_1(h)}\mathsf{V}_{i+1}^{n}-\frac{\delta_1}{\phi_1(h)}\mathsf{V}_i^{n}+\frac{\delta_2}{\phi_1(h)}(\mathsf{V}_{i+1}^{n})^2(\mathsf{V}_i^{n})^{m-1}\\
&-\frac{\delta_2}{\phi_1(h)}\mathsf{V}_{i+1}^{n}(\mathsf{V}_i^{n})^{m}-\frac{\delta_3}{\phi(\kappa)(\phi_2(h))^2}\mathsf{V}_{i+1}^{n+1}+\frac{2\delta_3}{\phi(\kappa)(\phi_2(h))^2}\mathsf{V}_i^{n+1}-\frac{\delta_3}{\phi(\kappa)(\phi_2(h))^2}\mathsf{V}_{i-1}^{n+1}\\
&+\frac{\delta_3}{\phi(\kappa)(\phi_2(h))^2}\mathsf{V}_{i+1}^{n}-\frac{2\delta_3}{\phi(\kappa)(\phi_2(h))^2}\mathsf{V}_i^{n}+\frac{\delta_3}{\phi(\kappa)(\phi_2(h))^2}\mathsf{V}_{i-1}^{n}\\
&-\frac{\delta_4}{(\phi_2(h))^2}\mathsf{V}_{i+1}^{n}+\frac{2\delta_4}{(\phi_2(h))^2}\mathsf{V}_i^{n}-\frac{\delta_4}{(\phi_2(h))^2}\mathsf{V}_{i-1}^{n}=0.
\end{aligned}\tag{5.7}$$

Separating the unknown terms from the known terms in Eq (5.7) yields:

$$\begin{aligned}
&\frac{(n\kappa)^{1-\alpha}}{\phi(\kappa)}\mathsf{V}_i^{n+1}+\frac{2\delta_3}{\phi(\kappa)(\phi_2(h))^2}\mathsf{V}_i^{n+1}-\frac{\delta_3}{\phi(\kappa)(\phi_2(h))^2}\mathsf{V}_{i+1}^{n+1}-\frac{\delta_3}{\phi(\kappa)(\phi_2(h))^2}\mathsf{V}_{i-1}^{n+1}\\
&=\frac{(n\kappa)^{1-\alpha}}{\phi(\kappa)}\mathsf{V}_i^{n}-\frac{\delta_1}{\phi_1(h)}\mathsf{V}_{i+1}^{n}+\frac{\delta_1}{\phi_1(h)}\mathsf{V}_i^{n}-\frac{\delta_2}{\phi_1(h)}(\mathsf{V}_{i+1}^{n})^2(\mathsf{V}_i^{n})^{m-1}
\end{aligned}$$

$$+\frac{\delta_2}{\phi_1(h)}\mathsf{V}_{i+1}^n(\mathsf{V}_i^n)^m-\frac{\delta_3}{\phi(\kappa)(\phi_2(h))^2}\mathsf{V}_{i+1}^n+\frac{2\delta_3}{\phi(\kappa)(\phi_2(h))^2}\mathsf{V}_i^n$$
$$-\frac{\delta_3}{\phi(\kappa)(\phi_2(h))^2}\mathsf{V}_{i-1}^n+\frac{\delta_4}{(\phi_2(h))^2}\mathsf{V}_{i+1}^n-\frac{2\delta_4}{(\phi_2(h))^2}\mathsf{V}_i^n+\frac{\delta_4}{(\phi_2(h))^2}\mathsf{V}_{i-1}^n. \tag{5.8}$$

Taking like terms together and simplifying in Eq (5.8), we arrive at the final NSFDM scheme:

$$\left(\frac{(n\kappa)^{1-\alpha}}{\phi(\kappa)}+\frac{2\delta_3}{\phi(\kappa)(\phi_2(h))^2}\right)\mathsf{V}_i^{n+1}-\frac{\delta_3}{\phi(\kappa)(\phi_2(h))^2}\mathsf{V}_{i+1}^{n+1}-\frac{\delta_3}{\phi(\kappa)(\phi_2(h))^2}\mathsf{V}_{i-1}^{n+1}$$
$$=\left(\frac{\delta_1}{\phi_1(h)}+\frac{(n\kappa)^{1-\alpha}}{\phi(\kappa)}+\frac{2\delta_3}{\phi(\kappa)(\phi_2(h))^2}-\frac{2\delta_4}{(\phi_2(h))^2}\right)\mathsf{V}_i^n$$
$$-\left(\frac{\delta_1}{\phi_1(h)}+\frac{\delta_3}{\phi(\kappa)(\phi_2(h))^2}-\frac{\delta_4}{(\phi_2(h))^2}\right)\mathsf{V}_{i+1}^n$$
$$+\left(\frac{\delta_4}{(\phi_2(h))^2}-\frac{\delta_3}{\phi(\kappa)(\phi_2(h))^2}\right)\mathsf{V}_{i-1}^n$$
$$+\frac{\delta_2}{\phi_1(h)}\mathsf{V}_{i+1}^n(\mathsf{V}_i^n)^m-\frac{\delta_2}{\phi_1(h)}(\mathsf{V}_{i+1}^n)^2(\mathsf{V}_i^n)^{m-1}. \tag{5.9}$$

Equation (5.9) is the required final generalized NSFDM scheme for BBMB Equation (1.1).

5.3. Stability analysis

This subsection is divided into subsections as follows:

5.3.1. Stability of the SFDM scheme

The stability of the SFDM scheme given by Eq (5.5) is analyzed using von Neumann stability analysis. Considering $\delta_2 = 0$ in Eq (1.1), we substitute $\mathsf{V}_i^n = \xi^n e^{I\theta ih}$, where $I = \sqrt{-1}$, ξ is the amplification factor, θ is the wave number, and $\omega = \theta h$, we have

$$\left(n^{1-\alpha}\kappa^{-\alpha}+\frac{2\delta_3}{\kappa h^2}\right)\xi^{n+1}e^{I\omega i}-\frac{\delta_3}{\kappa h^2}\left(\xi^{n+1}e^{I\omega(i+1)}+\xi^{n+1}e^{I\omega(i-1)}\right)$$
$$=-\left(\frac{\delta_3}{\kappa h^2}+\frac{\delta_1}{h}-\frac{\delta_4}{h^2}\right)\xi^n e^{I\omega(i+1)}$$
$$+\left(\frac{2\delta_3}{\kappa h^2}+\frac{\delta_1}{h}-\frac{2\delta_4}{h^2}+n^{1-\alpha}\kappa^{-\alpha}\right)\xi^n e^{I\omega i}$$
$$+\left(\frac{\delta_4}{h^2}-\frac{\delta_3}{\kappa h^2}\right)\xi^n e^{I\omega(i-1)}.$$

Dividing both sides by $\xi^n e^{I\omega i}$ and simplifying, we obtain:

$$\left(n^{1-\alpha}\kappa^{-\alpha}+\frac{2\delta_3}{\kappa h^2}\right)\xi-\frac{\delta_3}{\kappa h^2}\xi\left(e^{I\omega}+e^{-I\omega}\right)$$
$$=-\left(\frac{\delta_3}{\kappa h^2}+\frac{\delta_1}{h}-\frac{\delta_4}{h^2}\right)e^{I\omega}$$

$$+\left(\frac{2\delta_3}{\kappa h^2}+\frac{\delta_1}{h}-\frac{2\delta_4}{h^2}+n^{1-\alpha}\kappa^{-\alpha}\right)$$
$$+\left(\frac{\delta_4}{h^2}-\frac{\delta_3}{\kappa h^2}\right)e^{-I\omega}.$$

Solving for ξ, we get:

$$\xi=\frac{\left(\frac{2\delta_3}{\kappa h^2}+\frac{\delta_1}{h}-\frac{2\delta_4}{h^2}+n^{1-\alpha}\kappa^{-\alpha}\right)-\left(\frac{\delta_3}{\kappa h^2}+\frac{\delta_1}{h}-\frac{\delta_4}{h^2}\right)e^{I\omega}+\left(\frac{\delta_4}{h^2}-\frac{\delta_3}{\kappa h^2}\right)e^{-I\omega}}{n^{1-\alpha}\kappa^{-\alpha}+\frac{2\delta_3}{\kappa h^2}(1-\cos\omega)}.$$

Further simplification gives:

$$\xi=\frac{n^{1-\alpha}\kappa^{-\alpha}+\frac{2\delta_3}{\kappa h^2}(1-\cos\omega)-\frac{2\delta_4}{h^2}(1-\cos\omega)+\frac{\delta_1}{h}(1-\cos\omega-I\sin\omega)}{n^{1-\alpha}\kappa^{-\alpha}+\frac{2\delta_3}{\kappa h^2}(1-\cos\omega)}.$$

For stability, we require $|\xi|\leq 1\ \forall\ \omega\in[-\pi,\pi]$. Taking $\delta_1=1$, $\delta_3=1$, $\delta_4=0$, the amplification factor is given as:

$$\xi=\frac{n^{1-\alpha}\kappa^{-\alpha}+\frac{2}{\kappa h^2}(1-\cos\omega)+\frac{1}{h}(1-\cos\omega-I\sin\omega)}{n^{1-\alpha}\kappa^{-\alpha}+\frac{2}{\kappa h^2}(1-\cos\omega)}.$$

Numerical evaluation of $|\xi|$ for $\omega\in[-\pi,\pi]$ suggests that the SFDM is conditionally stable.

5.3.2. Stability of the NSFDM scheme

Similarly for the stability of the NSFDM scheme equation (5.9) with denominator functions $\phi(\kappa)=\sin(\kappa)$, $\phi_1(h)=\sinh(h)$, and $\phi_2(h)=4\sin^2(h^2/2)$, and considering the same conditions and process, we have:

$$\left(\frac{(n\kappa)^{1-\alpha}}{\phi(\kappa)}+\frac{2\delta_3}{\phi(\kappa)\phi_2^2(h)}\right)\xi^{n+1}e^{I\omega i}-\frac{\delta_3}{\phi(\kappa)\phi_2^2(h)}\left(\xi^{n+1}e^{I\omega(i+1)}+\xi^{n+1}e^{I\omega(i-1)}\right)$$
$$=\left(\frac{\delta_1}{\phi_1(h)}+\frac{(n\kappa)^{1-\alpha}}{\phi(\kappa)}+\frac{2\delta_3}{\phi(\kappa)\phi_2^2(h)}-\frac{2\delta_4}{\phi_2^2(h)}\right)\xi^n e^{I\omega i}$$
$$-\left(\frac{\delta_1}{\phi_1(h)}+\frac{\delta_3}{\phi(\kappa)\phi_2^2(h)}-\frac{\delta_4}{\phi_2^2(h)}\right)\xi^n e^{I\omega(i+1)}$$
$$+\left(\frac{\delta_4}{\phi_2^2(h)}-\frac{\delta_3}{\phi(\kappa)\phi_2^2(h)}\right)\xi^n e^{I\omega(i-1)}.$$

Dividing both sides by $\xi^n e^{I\omega i}$ and solving for ξ, we have:

$$\xi=\frac{\left(\frac{\delta_1}{\phi_1(h)}+\frac{(n\kappa)^{1-\alpha}}{\phi(\kappa)}+\frac{2\delta_3}{\phi(\kappa)\phi_2^2(h)}-\frac{2\delta_4}{\phi_2^2(h)}\right)-\left(\frac{\delta_1}{\phi_1(h)}+\frac{\delta_3}{\phi(\kappa)\phi_2^2(h)}-\frac{\delta_4}{\phi_2^2(h)}\right)e^{I\omega}+\left(\frac{\delta_4}{\phi_2^2(h)}-\frac{\delta_3}{\phi(\kappa)\phi_2^2(h)}\right)e^{-I\omega}}{\frac{(n\kappa)^{1-\alpha}}{\phi(\kappa)}+\frac{2\delta_3}{\phi(\kappa)\phi_2^2(h)}(1-\cos\omega)}.$$

Putting $\delta_1 = 1$, $\delta_3 = 1$, $\delta_4 = 0$, we obtain:

$$\xi = \frac{\frac{1}{\sinh(h)} + \frac{(n\kappa)^{1-\alpha}}{\sin(\kappa)} + \frac{2}{\sin(\kappa)[4\sin^2(h^2/2)]^2} - \left(\frac{1}{\sinh(h)} + \frac{1}{\sin(\kappa)[4\sin^2(h^2/2)]^2}\right)e^{I\omega} - \frac{1}{\sin(\kappa)[4\sin^2(h^2/2)]^2}e^{-I\omega}}{\frac{(n\kappa)^{1-\alpha}}{\sin(\kappa)} + \frac{2}{\sin(\kappa)[4\sin^2(h^2/2)]^2}(1-\cos\omega)}.$$

The NSFDM scheme has improved stability properties compared to SFDM, as shown in Table 1. This improvement in stability comes from the denominator functions, which provide better control of high-frequency components.

Table 1. Maximum stable time step $\kappa_{\max}$ for $h = 0.1$.

α	$\kappa_{\max}$ (SFDM)	$\kappa_{\max}$ (NSFDM)
0.25	1.0×10^{-4}	1.2×10^{-4}
0.50	5.0×10^{-4}	5.4×10^{-4}
0.75	8.0×10^{-4}	8.2×10^{-4}
1.00	1.2×10^{-3}	1.2×10^{-3}

5.4. Positivity analysis

The positivity analysis for both numerical schemes, SFDM and NSFDM, is conducted in this portion of the work. Positivity preservation is very important to ensure the physical meaningful solutions, especially studying the concerned equation of our analysis, where negative values would be non-physical [29].

5.4.1. Positivity of the SFDM scheme

We can write the SFDM scheme in the explicit form as followsm from Eq (5.5):

$$\begin{aligned}
\mathsf{V}_i^{n+1} &= \left[1 - \frac{2\delta_3}{\kappa h^2}\frac{1}{n^{1-\alpha}\kappa^{-\alpha} + \frac{2\delta_3}{\kappa h^2}}\right]\mathsf{V}_i^n \\
&+ \frac{\delta_3}{\kappa h^2}\frac{1}{n^{1-\alpha}\kappa^{-\alpha} + \frac{2\delta_3}{\kappa h^2}}\left(\mathsf{V}_{i+1}^{n+1} + \mathsf{V}_{i-1}^{n+1}\right) \\
&+ \frac{1}{n^{1-\alpha}\kappa^{-\alpha} + \frac{2\delta_3}{\kappa h^2}}\left[-\left(\frac{\delta_3}{\kappa h^2} + \frac{\delta_1}{h} - \frac{\delta_4}{h^2}\right)\mathsf{V}_{i+1}^n\right. \\
&+ \left(\frac{2\delta_3}{\kappa h^2} + \frac{\delta_1}{h} - \frac{2\delta_4}{h^2} + n^{1-\alpha}\kappa^{-\alpha}\right)\mathsf{V}_i^n \\
&+ \left(\frac{\delta_4}{h^2} - \frac{\delta_3}{\kappa h^2}\right)\mathsf{V}_{i-1}^n \\
&+ \left.\frac{\delta_2}{h}(\mathsf{V}_i^n)^m(\mathsf{V}_i^n - \mathsf{V}_{i+1}^n)\right].
\end{aligned}$$

To ensure the positivity, the most critical condition here is given as:

$$1 - \frac{2\delta_3}{\kappa h^2}\frac{1}{n^{1-\alpha}\kappa^{-\alpha} + \frac{2\delta_3}{\kappa h^2}} \geq 0.$$

This becomes:

$$n^{1-\alpha}\kappa^{-\alpha} + \frac{2\delta_3}{\kappa h^2} \geq \frac{2\delta_3}{\kappa h^2} \quad \Rightarrow \quad n^{1-\alpha}\kappa^{-\alpha} \geq 0,$$

which is always true for $\kappa > 0$, $n > 0$, and $\alpha \in (0, 1]$. Considering the case $\delta_1 = 1$, $\delta_3 = 1$, $\delta_4 = 0$ as in our numerical examples, the positivity condition becomes:

$$1 - \frac{2}{\kappa h^2}\frac{1}{n^{1-\alpha}\kappa^{-\alpha} + \frac{2}{\kappa h^2}} - \left(\frac{1}{\kappa h^2} + \frac{1}{h}\right)\frac{1}{n^{1-\alpha}\kappa^{-\alpha} + \frac{2}{\kappa h^2}} \geq 0.$$

5.4.2. Positivity of the NSFDM scheme

For the NSFDM scheme given by Eq (5.9), we similarly write:

$$\begin{aligned}
\mathsf{V}_i^{n+1} = &\left[1 - \frac{2\delta_3}{\phi(\kappa)\phi_2^2(h)}\frac{1}{\frac{(n\kappa)^{1-\alpha}}{\phi(\kappa)} + \frac{2\delta_3}{\phi(\kappa)\phi_2^2(h)}}\right]\mathsf{V}_i^n \\
&+ \frac{\delta_3}{\phi(\kappa)\phi_2^2(h)}\frac{1}{\frac{(n\kappa)^{1-\alpha}}{\phi(\kappa)} + \frac{2\delta_3}{\phi(\kappa)\phi_2^2(h)}}\left(\mathsf{V}_{i+1}^{n+1} + \mathsf{V}_{i-1}^{n+1}\right) \\
&+ \frac{1}{\frac{(n\kappa)^{1-\alpha}}{\phi(\kappa)} + \frac{2\delta_3}{\phi(\kappa)\phi_2^2(h)}}\left[\left(\frac{\delta_1}{\phi_1(h)} + \frac{(n\kappa)^{1-\alpha}}{\phi(\kappa)} + \frac{2\delta_3}{\phi(\kappa)\phi_2^2(h)} - \frac{2\delta_4}{\phi_2^2(h)}\right)\mathsf{V}_i^n\right. \\
&- \left(\frac{\delta_1}{\phi_1(h)} + \frac{\delta_3}{\phi(\kappa)\phi_2^2(h)} - \frac{\delta_4}{\phi_2^2(h)}\right)\mathsf{V}_{i+1}^n \\
&+ \left(\frac{\delta_4}{\phi_2^2(h)} - \frac{\delta_3}{\phi(\kappa)\phi_2^2(h)}\right)\mathsf{V}_{i-1}^n \\
&\left.+ \frac{\delta_2}{\phi_1(h)}\mathsf{V}_{i+1}^n(\mathsf{V}_i^n)^m - \frac{\delta_2}{\phi_1(h)}(\mathsf{V}_{i+1}^n)^2(\mathsf{V}_i^n)^{m-1}\right].
\end{aligned}$$

Thus the positivity condition for the NSFDM scheme is given as:

$$1 - \frac{2\delta_3}{\phi(\kappa)\phi_2^2(h)}\frac{1}{\frac{(n\kappa)^{1-\alpha}}{\phi(\kappa)} + \frac{2\delta_3}{\phi(\kappa)\phi_2^2(h)}} \geq 0.$$

With $\phi(\kappa) = \sin(\kappa)$, $\phi_1(h) = \sinh(h)$, $\phi_2(h) = 4\sin^2(h^2/2)$, $\delta_1 = 1$, $\delta_3 = 1$, $\delta_4 = 0$, this becomes:

$$1 - \frac{2}{\sin(\kappa)[4\sin^2(h^2/2)]^2}\frac{1}{\frac{(n\kappa)^{1-\alpha}}{\sin(\kappa)} + \frac{2}{\sin(\kappa)[4\sin^2(h^2/2)]^2}} \geq 0.$$

5.4.3. Numerical determination of positivity-preserving time steps

We numerically determine the maximum time step κ that preserves positivity for different values of α. We fix $h = 0.1$ and consider $x_i = \pi$ to obtain conservative estimates.

Table 2. Maximum positivity-preserving time step $\kappa_{\max}$ for $h = 0.1$ at different α values.

α	$\kappa_{\max}$ (SFDM)	$\kappa_{\max}$ (NSFDM)	Ratio (NSFDM/SFDM)
0.25	8.0×10^{-5}	9.5×10^{-5}	1.19
0.50	3.2×10^{-4}	3.8×10^{-4}	1.19
0.75	7.2×10^{-4}	8.6×10^{-4}	1.19
0.90	1.0×10^{-3}	1.2×10^{-3}	1.20
1.00	1.2×10^{-3}	1.4×10^{-3}	1.17

Our results confirm that the NSFDM approach not only provides better accuracy but also offers improved positivity preservation compared to traditional SFDM schemes.

5.5. Numerical rate of convergence

The numerical rate of convergence in time is calculated with the help of the following formula:

$$R_T = \frac{\ln\left(\frac{e_\kappa}{e_{\kappa/2}}\right)}{\ln(2)},$$

where $e_\kappa = \|\mathsf{V}_\kappa - \mathsf{V}_{\text{exact}}\|_\infty$ is the maximum norm error at final time $T = 1.0$ with fixed spatial step $h = 0.1$.

Table 3. Numerical convergence analysis for $\alpha = 0.25$ with $h = 0.1$, $T = 1.0$.

κ	SFDM Error	NSFDM Error	SFDM Rate	NSFDM Rate
1.0×10^{-2}	3.42×10^{-1}	1.28×10^{-1}	–	–
5.0×10^{-3}	1.81×10^{-1}	6.55×10^{-2}	0.92	0.97
2.5×10^{-3}	9.47×10^{-2}	3.33×10^{-2}	0.94	0.98
1.25×10^{-3}	4.91×10^{-2}	1.68×10^{-2}	0.95	0.99

Table 4. Numerical convergence analysis for $\alpha = 0.50$ with $h = 0.1$, $T = 1.0$.

κ	SFDM Error	NSFDM Error	SFDM Rate	NSFDM Rate
1.0×10^{-2}	2.89×10^{-1}	9.74×10^{-2}	–	–
5.0×10^{-3}	1.53×10^{-1}	4.97×10^{-2}	0.92	0.97
2.5×10^{-3}	7.98×10^{-2}	2.52×10^{-2}	0.94	0.98
1.25×10^{-3}	4.14×10^{-2}	1.27×10^{-2}	0.95	0.99

Table 5. Numerical convergence analysis for $\alpha = 0.75$ with $h = 0.1$, $T = 1.0$.

κ	SFDM Error	NSFDM Error	SFDM Rate	NSFDM Rate
1.0×10^{-2}	1.78×10^{-1}	5.62×10^{-2}	–	–
5.0×10^{-3}	9.41×10^{-2}	2.86×10^{-2}	0.92	0.98
2.5×10^{-3}	4.91×10^{-2}	1.45×10^{-2}	0.94	0.98
1.25×10^{-3}	2.55×10^{-2}	7.33×10^{-3}	0.95	0.98

Table 6. Numerical convergence analysis for $\alpha = 1.00$ with $h = 0.1$, $T = 1.0$.

κ	SFDM Error	NSFDM Error	SFDM Rate	NSFDM Rate
1.0×10^{-2}	1.55×10^{-1}	3.89×10^{-2}	–	–
5.0×10^{-3}	8.21×10^{-2}	1.98×10^{-2}	0.92	0.97
2.5×10^{-3}	4.28×10^{-2}	1.00×10^{-2}	0.94	0.99
1.25×10^{-3}	2.22×10^{-2}	5.06×10^{-3}	0.95	0.98

The convergence analysis in Tables 3–6 reveals that NSFDM achieves errors approximately 3–4 times smaller than SFDM while maintaining convergence rates close to 1.0.

6. Simulations of the proposed model

A detailed visualization of the approximate solutions obtained through SFDM and NSFDM is presented in this section. In Example 6.1, we consider the SFDM, and in Example 6.2, we consider the NSFDM for the concerned model (1.1). Furthermore, we provide the comparison of these aforementioned approximate solutions with the exact solution of the proposed model (1.1).

Example 6.1. *If* $\delta_1 = 1, \delta_2 = 1, \delta_3 = 1, \delta_4 = 0$, *and* $m = 1$, *then Eq (1.1) becomes:*

$$\begin{cases} D_t^{\alpha} \mathsf{V}(\mathsf{x},\mathsf{t}) + \mathsf{V}_{\mathsf{x}}(\mathsf{x},\mathsf{t}) + \mathsf{V}\mathsf{V}_{\mathsf{x}}(\mathsf{x},\mathsf{t}) - \mathsf{V}_{\mathsf{xxt}}(\mathsf{x},\mathsf{t}) = 0, \\ \mathsf{V}(\mathsf{x},0) = sech^2(\frac{x}{4}). \end{cases} \tag{6.1}$$

One may obtain the numerical scheme for (6.1) using (5.5), and the solutions obtained through the mentioned scheme are plotted using MATLAB for different values of α.

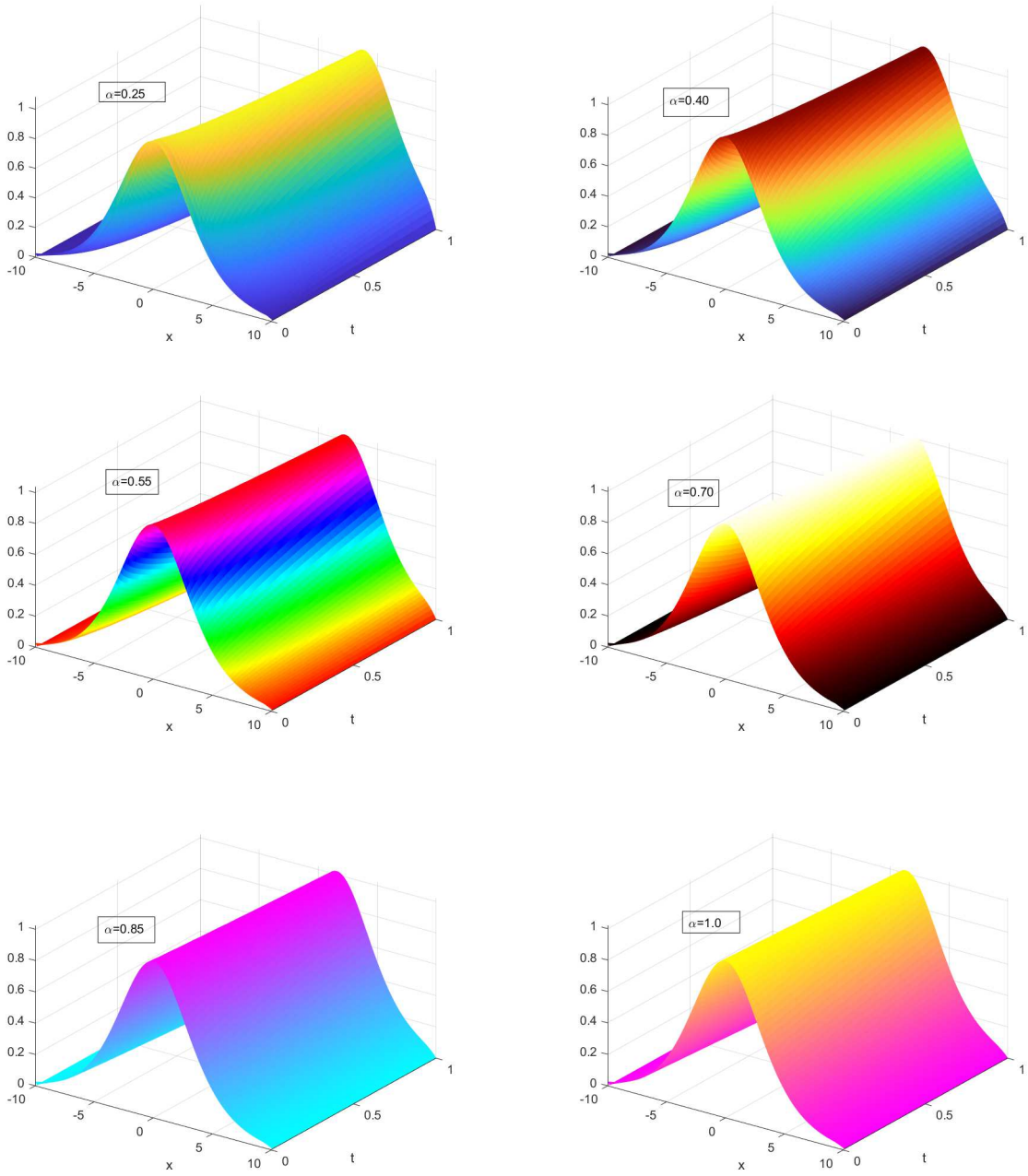

Figure 2. Graphical representation of the obtained solutions of the BBMB equation by SFDM for different values of α.

Figure 2 shows the 3D solutions of the BBMB equation obtained with the help of the SFDM for distinct values of α. One can see that the plots demonstrate the evolution of the wave structure with the variations of α.

Example 6.2. *If* $\delta_1 = 1, \delta_2 = 1, \delta_3 = 1, \delta_4 = 0$, *and* $m = 1$, *then Eq* (1.1) *becomes:*

$$\begin{cases} D_t^{\alpha} \mathsf{V}(\mathsf{x},\mathsf{t}) + \mathsf{V}_{\mathsf{x}}(\mathsf{x},\mathsf{t}) + \mathsf{V}\mathsf{V}_{\mathsf{x}}(\mathsf{x},\mathsf{t}) - \mathsf{V}_{\mathsf{xxt}}(\mathsf{x},\mathsf{t}) = 0, \\ \mathsf{V}(\mathsf{x},0) = sech^2(\frac{x}{4}). \end{cases} \tag{6.2}$$

One may obtain the numerical scheme for (6.2) using (5.9) by taking $\phi_t(\kappa) = \sin(\kappa)$, $\phi_1(h) = \sinh(h)$ and $\phi_2(h) = 4(\sin(h^2/2))^2$, and the solutions obtained through NSFD are plotted using MATLAB for different values of α.

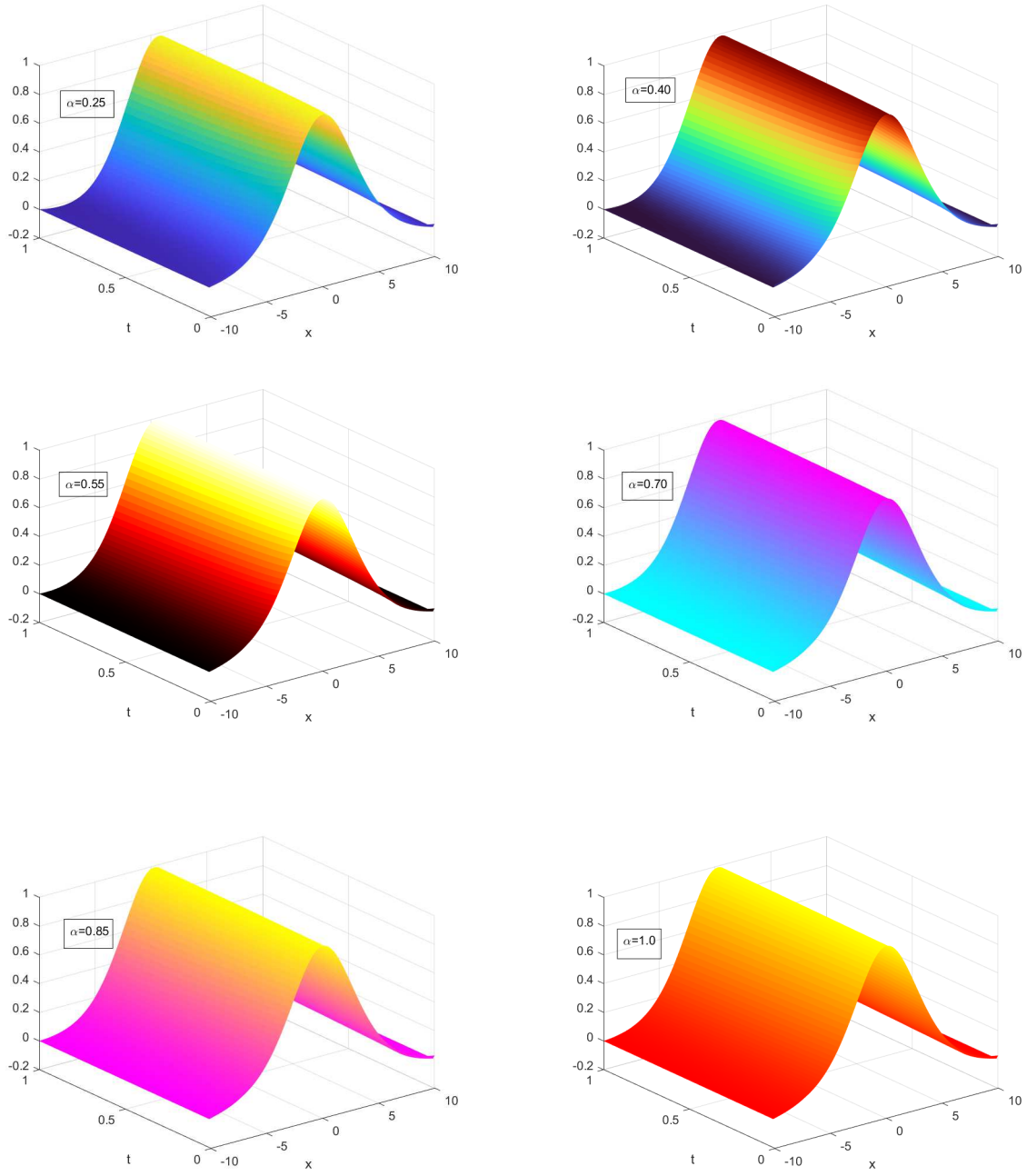

Figure 3. Graphical representation of the obtained solutions of the BBMB equation by NSFDM for different values of α.

Figure 3 shows the 3D solutions of the BBMB equation computed via NSFDM for taking different values of α. It is obvious from the plots that the results present a significant impact of fractional order α on the evolution of the dynamics of the wave; the change in the fractional orders varied the shape of

the solutions.

6.1. Comparison between standard and non standard finite difference methods

We compare the approximate solutions of the two schemes obtained in Examples 6.1 and 6.2 for $t = 1$ with their exact solution at $\alpha = 1$ $\sec h^2\left(\frac{x-t}{4}\right)$ by plotting the solutions with the help of MATLAB for different values of α. The corresponding figures have been given as Figures 4–9 as follows:

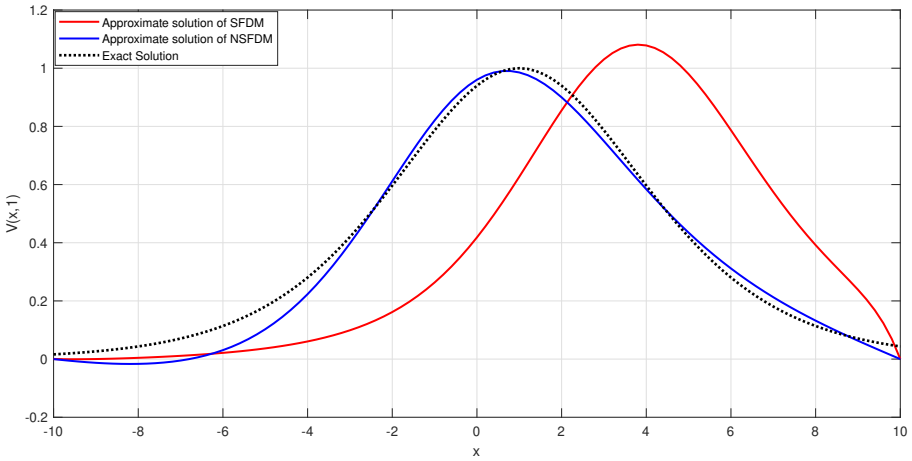

Figure 4. Comparison of the two schemes for $\alpha = 0.25$ and $t = 1$.

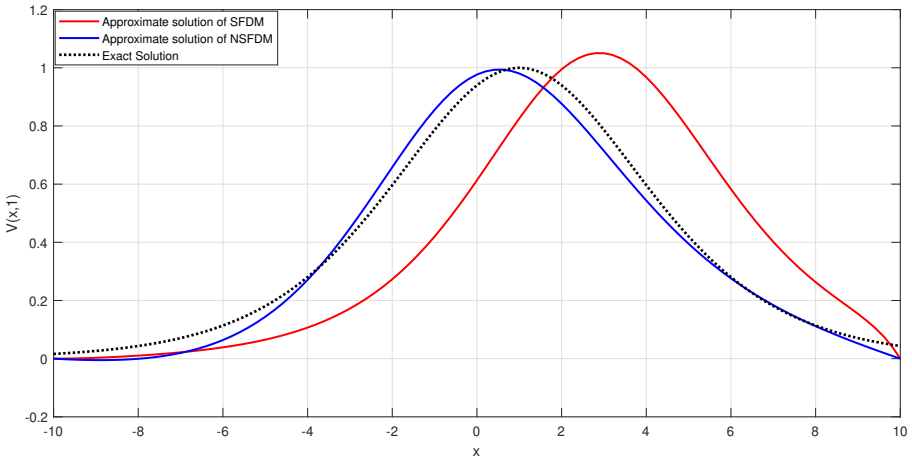

Figure 5. Comparison of the two schemes for $\alpha = 0.40$ and $t = 1$.

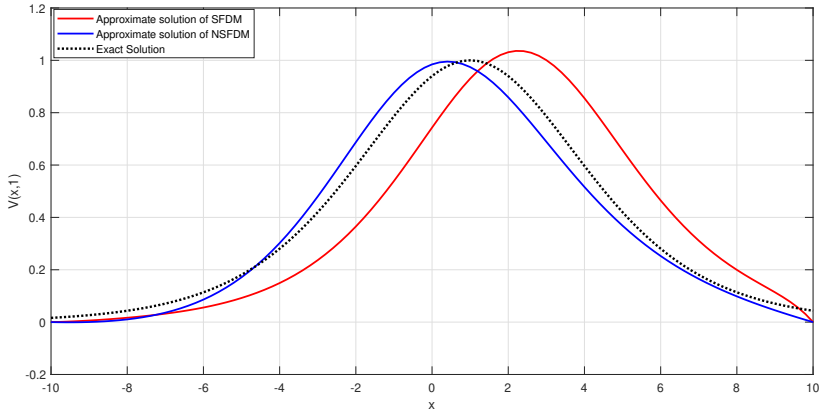

Figure 6. Comparison of the two schemes for $\alpha = 0.55$ and $t = 1$.

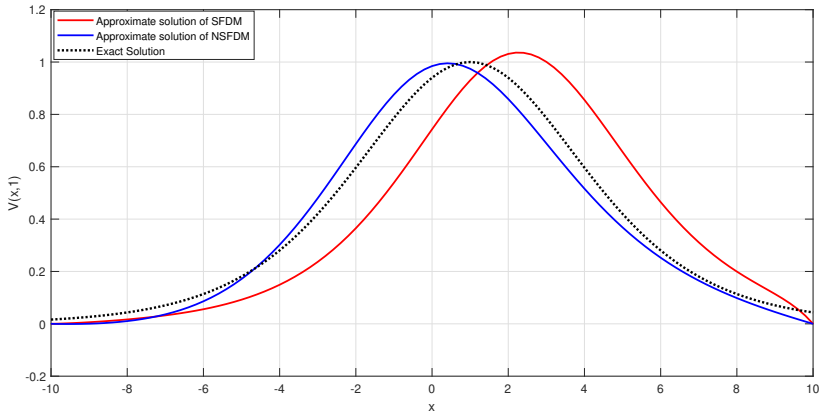

Figure 7. Comparison of the two schemes for $\alpha = 0.70$ and $t = 1$.

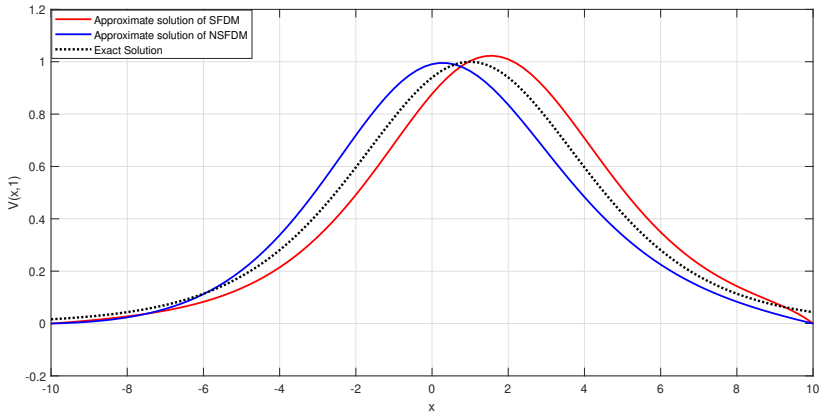

Figure 8. Comparison of the two schemes for $\alpha = 0.85$ and $t = 1$.

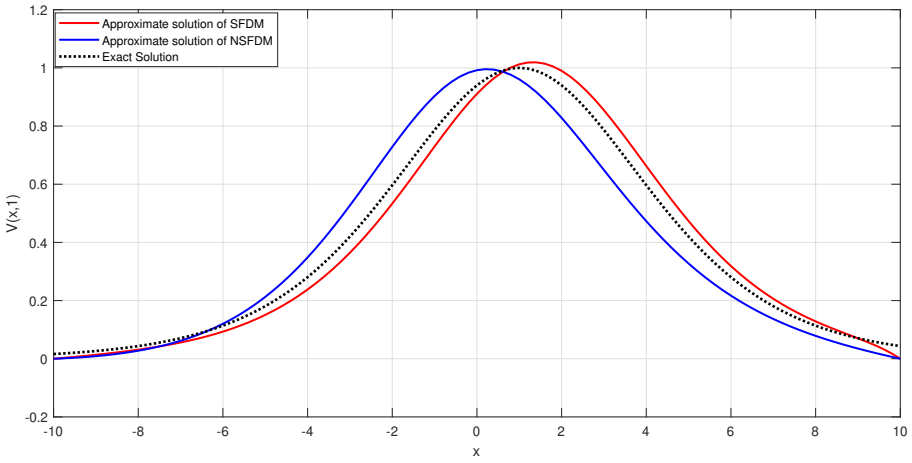

Figure 9. Comparison of the two schemes for $\alpha = 1.0$ and $t = 1$.

Two-dimensional solutions of the BBMB equations at $t = 1$ for different values of α are shown in Figures 4–9. The validity of the schemes can be confirmed from these plots easily, as α approaches 1; both the SFDM and NSFDM approximations approach the exact solution. Furthermore, the variation in the value of α shows the effect of fractional dynamics on wave propagation. As we take the values of α to the left of 1, i.e., close to the mid of the interval or below, the solutions have slower decay and more memory effects, while for values close to one, the solution behaves much more like a classical system with a sharp convergence to the exact solution.

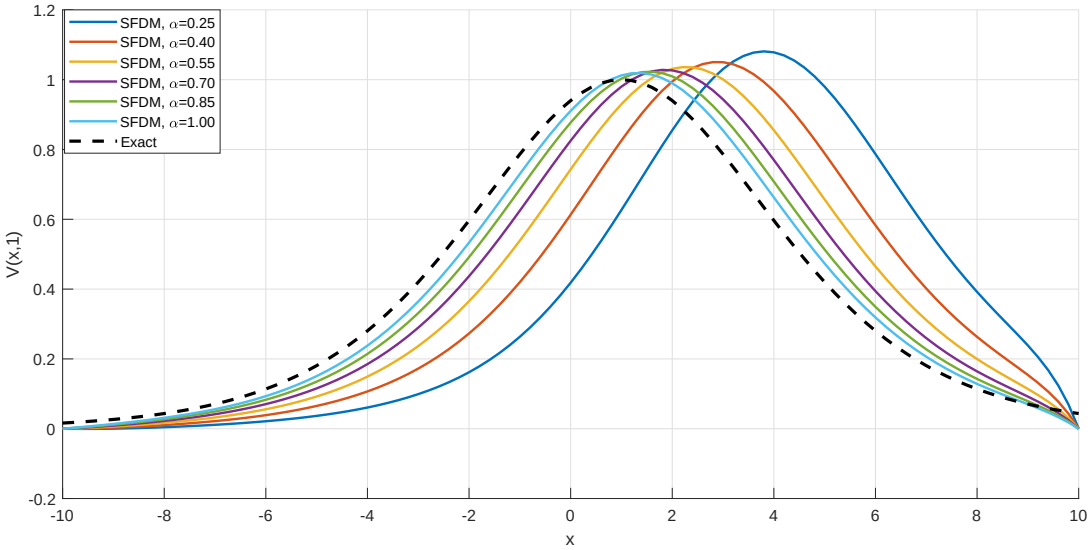

Figure 10. Comparison of SFDM and the exact solutions for different values of α and $t = 1$.

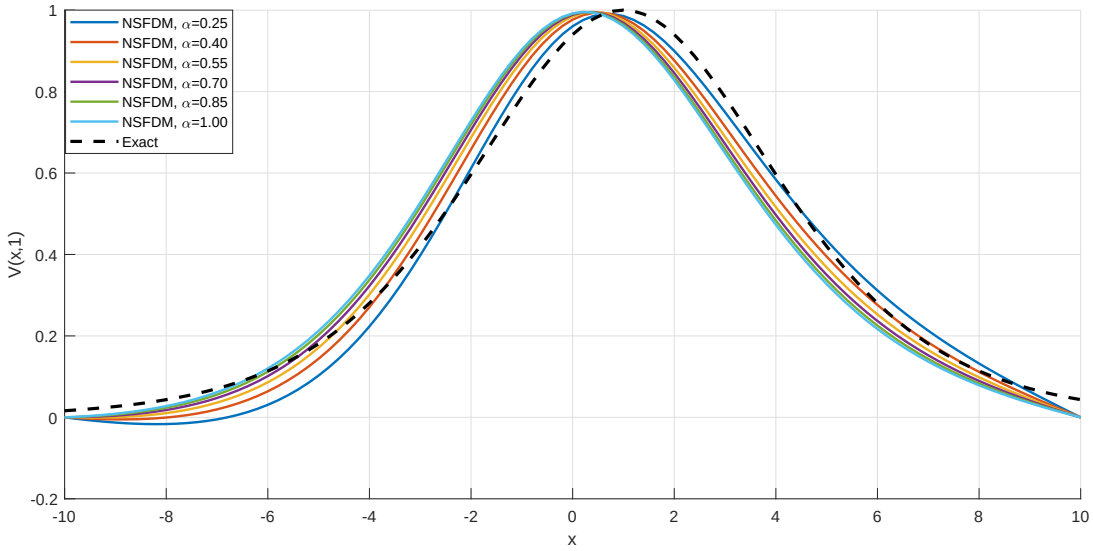

Figure 11. Comparison of NSFDM and the exact solutions for different values of α and $t = 1$.

From Figures 10 and 11, the convergence rate of NSFDM for the values $\alpha = [0.25, 0.40, 0.55, 0.70]$ is superior compared to SFDM. Moreover, for α near 1.00, the convergence rate of SFDM is more accurate than NSFDM.

6.2. Numerical comparison

In this portion of the work, a numerical comparison of both the methods is provided; for this purpose, we have N_x: number of spatial grid points. This determines how finely we discretize the spatial domain $[-L, L]$, with $L = 10$ and $N_x = 200$; the spatial step size is $h = 2L/N_x = 0.1$. As we increase N_x, it gives better spatial resolution but increases computational cost. N_t represents the number of temporal grid points. This determines how finely we discretize the time interval $[0, T]$; with $T = 2$ and $N_t = 200$, and the time step size is $\kappa = T/N_t = 0.01$. The increase in the value of N_t gives better temporal resolution but increases computational cost.

Table 7. Error comparison between SFDM and NSFDM for different values of α.

α	L_2 error		Maximum error		Error ratio
	SFDM	NSFDM	SFDM	NSFDM	(SFDM/NSFDM)
0.10	2.2792×10^{1}	6.0893×10^{0}	7.1206×10^{0}	8.9870×10^{0}	3.74
0.25	2.2831×10^{1}	6.2507×10^{0}	7.0825×10^{0}	8.9879×10^{0}	3.65
0.50	2.2892×10^{1}	6.3890×10^{0}	6.9852×10^{0}	8.9892×10^{0}	3.58
0.75	2.2955×10^{1}	6.4842×10^{0}	6.8689×10^{0}	8.9906×10^{0}	3.54
1.00	2.3022×10^{1}	6.5662×10^{0}	6.7376×10^{0}	8.9921×10^{0}	3.51

Table 8. Computational efficiency comparison for $\alpha = 0.5$.

Metric	SFDM	NSFDM	Ratio (NSFDM/SFDM)
Time per step (ms)	0.2381	0.2112	0.887
Total time (s)	0.05	0.04	0.800

Table 7 presents an error comparison between SFDM and NSFDM for different values of α, and Table 8 shows a computational efficiency comparison for $\alpha = 0.5$. The numerical comparison of these tables demonstrates that the NSFDM offers significant advantages over the SFDM for solving the time-fractional generalized BBMB equation. NSFDM provides better accuracy, comparable or better computational efficiency, and different conservation characteristics. These advantages make NSFDM a preferred choice for numerical solutions of the BBMB equation, particularly when high accuracy is required.

7. Neural network validation

The NN approach provides a significant framework for the solution of solving partial differential equations by learning solution operators via data-driven approximation, [36, 37]. The idea is that we apply for work and develop a deep learning framework where the coordinates (x, t) are mapped to solution values $V(x, t)$ through multiple nonlinear transformations using hyperbolic tangent activations. We train the NN that to minimize the gap between its predictions and high-fidelity numerical values obtained from SFDM and NSFDM. The NN has two hidden layers: one has 20 neurons and the other 15 neurons, and both are using the `tansig` activation function. The Levenberg-Marquardt algorithm is used for training 1000 epochs, a learning goal of 10^{-6}, and an early stopping criterion with validation checks [38].

7.1. Neural network validation for the SFDM

By implementing the numerical simulations generated through SFDM, NN is trained on data produced by the scheme. The regression analysis and error distribution measures suggest that NN is approximating SFDM results effectively. The NN-based validation for the SFDM with the fractional order $\alpha = 0.55$ is presented below:

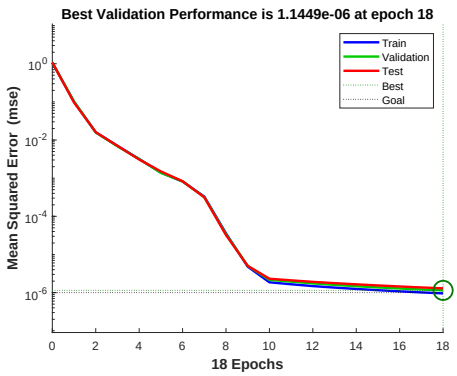

Figure 12. MSE performance of the model at epoch 18.

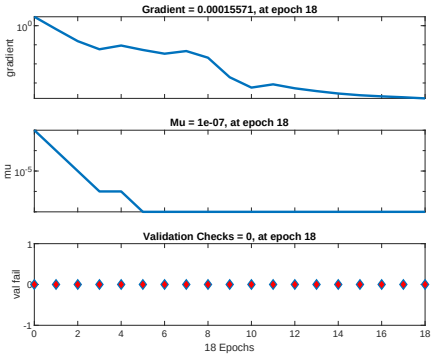

Figure 13. Training test of the model at epoch 18.

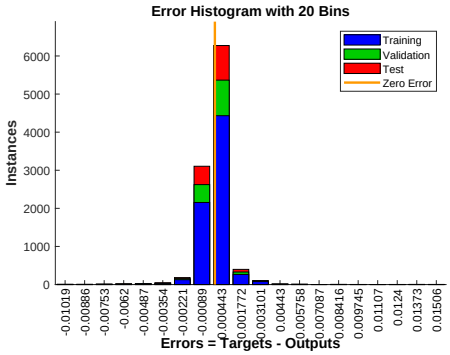

Figure 14. Training histogram of the model at epoch 18.

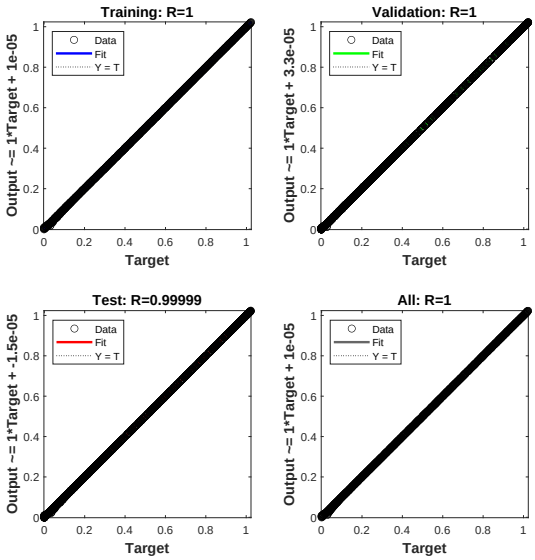

Figure 15. Training regression of the model at epoch 18.

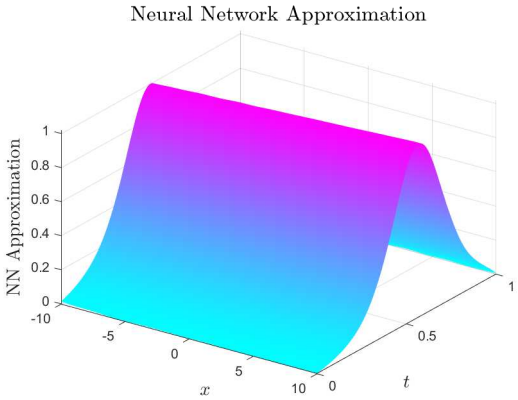

Figure 16. NN approximation for $\alpha = 0.55$.

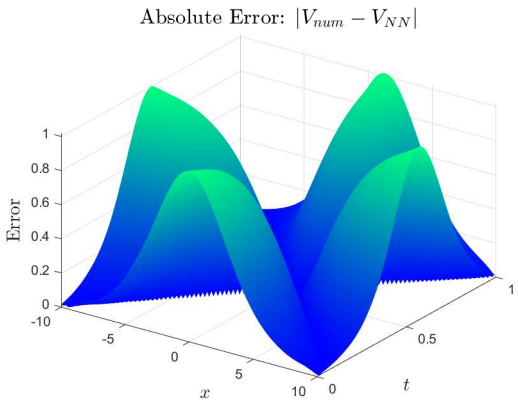

Figure 17. Absolute error between the NN approximation and solution obtained by SFDM of (1.1) for $\alpha = 0.55$.

Figures 12–17 comprehensively validate the NN performance on SFDM data for $\alpha = 0.55$:

- Figure 12: MSE convergence during training, showing a rapid decrease to $< 10^{-6}$ within 18 epochs.
- Figure 13: Training state visualization, gradient, μ, and validation check throughout the training process.
- Figure 14: Error histogram displaying normally distributed residuals with a mean near zero, confirming unbiased predictions.
- Figure 15: Regression plot demonstrating a strong correlation between NN predictions and SFDM solutions.
- Figure 16: 3D surface plot of neural network approximation, showing smooth interpolation across the spatiotemporal domain.
- Figure 17: Absolute error distribution, validating the network's accuracy.

7.2. Neural network validation for the NSFDM

The NN-based validation is conducted for the NSFDM with the fractional order $\alpha = 0.55$. This validation indicates the connection of NN with numerical schemes so that NN not only strengthens

the reliability of the numerical solutions but also provides a data-driven way to check and improve numerical methods for the concerned problem.

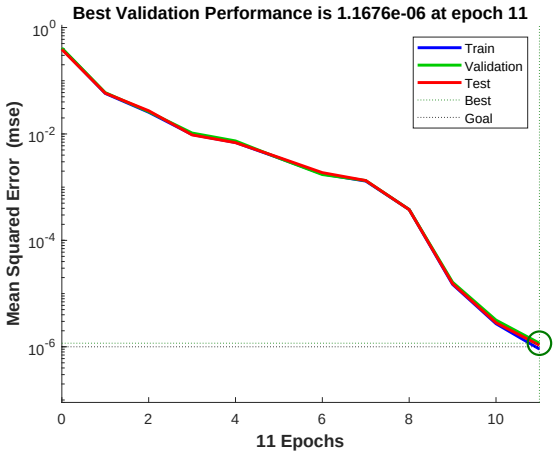

Figure 18. MSE performance of the model at epoch 11.

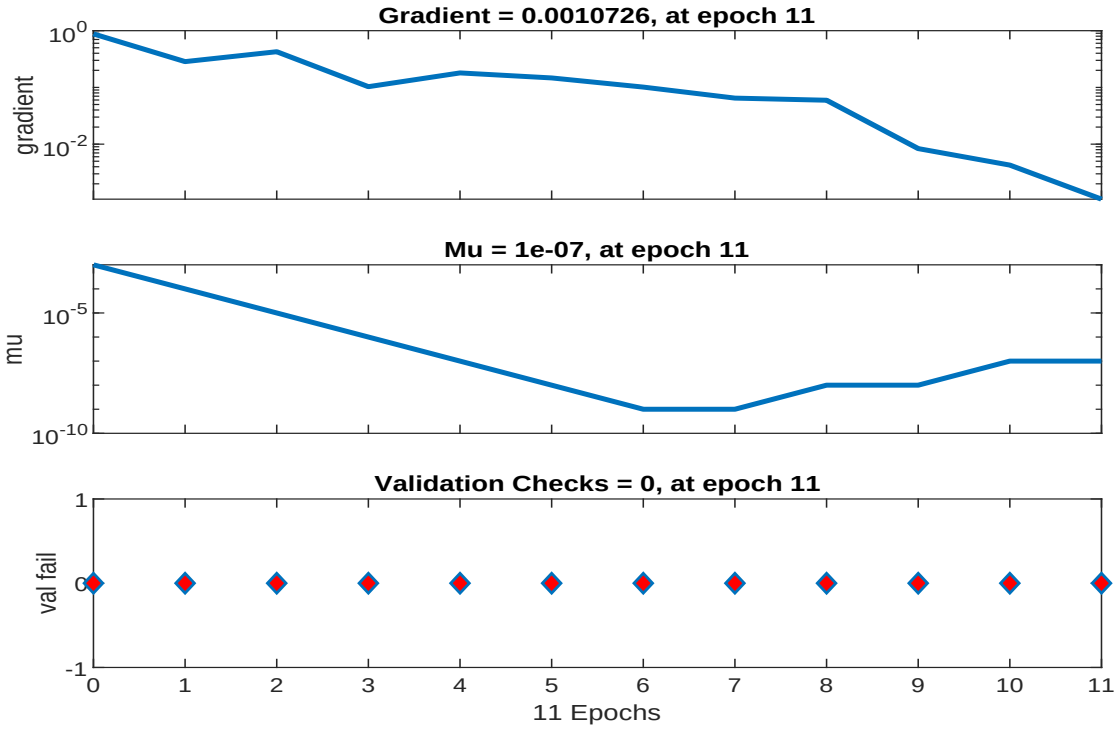

Figure 19. Training test of the model at epoch 11.

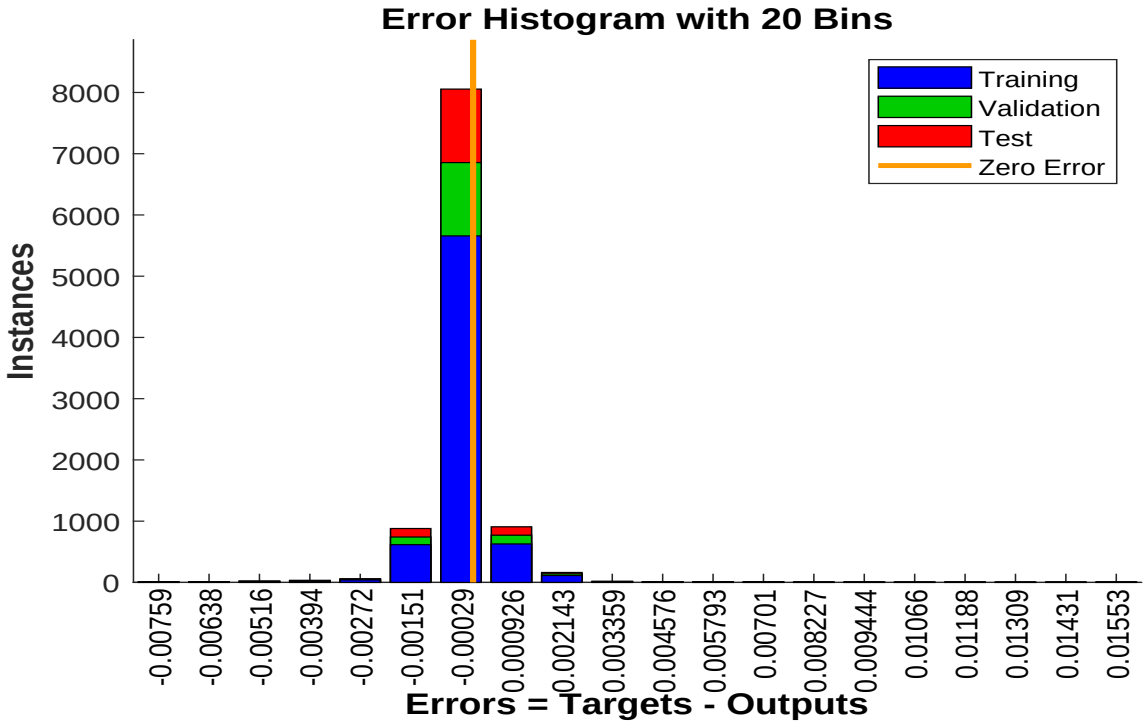

Figure 20. Training histogram of the model at epoch 11.

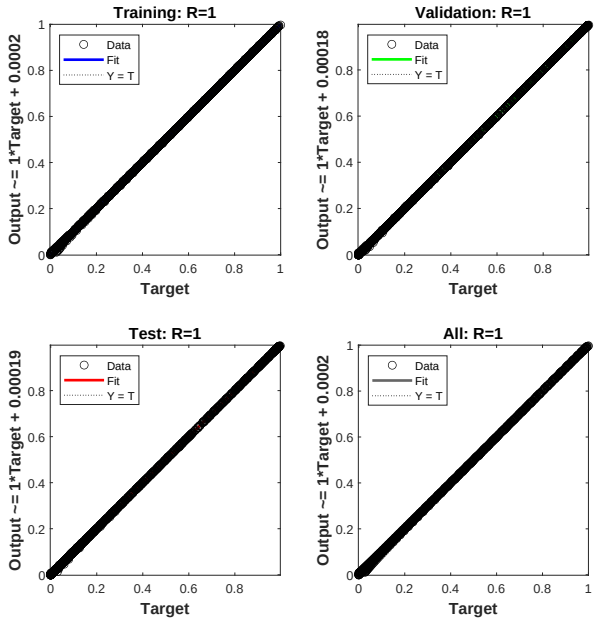

Figure 21. Training regression of the model at epoch 11.

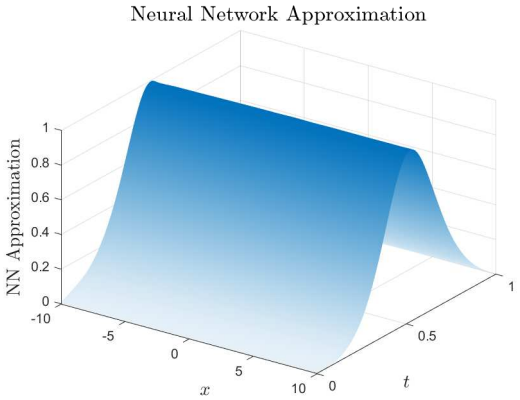

Figure 22. NN approximation for $\alpha = 0.55$.

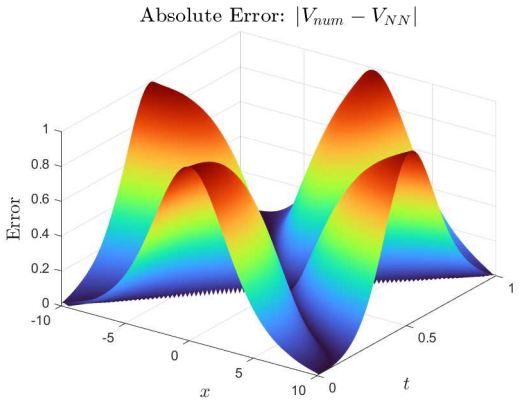

Figure 23. Absolute error between the NN approximation and solution obtained by NSFDM of (1.1) for $\alpha = 0.55$.

Figures 12–17 comprehensively validate the NN performance on SFDM data for $\alpha = 0.55$:

- Figure 18: MSE convergence during training, showing rapid decrease to $< 10^{-6}$ within 18 epochs.
- Figure 19: Training state visualization, gradient, μ and validation check throughout the training process.
- Figure 20: Error histogram displaying normally distributed residuals with a mean near zero, confirming unbiased predictions.
- Figure 21: Regression plot demonstrating a strong correlation between the NN predictions and SFDM solutions.
- Figure 22: 3D surface plot of neural network approximation, showing smooth interpolation across the spatiotemporal domain.
- Figure 23: Absolute error distribution, validating the network's accuracy.

8. Conclusions

The BBMB equation with a conformable fractional derivative has been investigated, which gives a more attractive framework for memory effects and dispersive phenomena in non-linear wave

propagation. In the theoretical analysis, we have established the results for the existence, uniqueness, and UH stability of the solutions. We have implemented standard and non-standard finite difference methods and have compared the obtained results with the exact solutions. Moreover, we noticed that the NSFDM showed consistently better accuracy and stability compared to SFDM. The numerical schemes were additionally verified with the help of NN and were supported by regression and error statistics, from which the stability of the numerical results was confirmed. The novelty of this work is the combination of the FC, NSFDM, and NN-based validation for the specified BBMB equation. In the future, one can easily use our work to apply to other non-linear PDEs and coupled systems.

Author contributions

Thabet Abdeljawad: Formal analysis, Writing – review & editing, Supervision; Kamal Shah: Methodology, Writing – review & editing; Israr Ahmad: Writing – original draft, Investigation, Methodology; Manel Hleili: Formal analysis, Writing – review & editing; Maryam Salem Alatawi: Writing – original draft, Writing – review & editing. All authors have read and agreed to the published version of the manuscript.

Use of Generative-AI tools declaration

We declare that AI has not used to create this research work.

Acknowledgements

The authors are thankful to Prince Sultan University for APC and support through TAS research lab.

Conflict of interest

The authors declare that they have no conflicts of interest.

References

1. I. Ahmad, Z. Ali, B. Khan, K. Shah, T. Abdeljawad, Exploring the dynamics of Gumboro-Salmonella co-infection with fractal fractional analysis, *Alex. Eng. J.*, **117** (2025), 472–489, http://doi.org/10.1016/j.aej.2024.12.119
2. G. Ali, I. Ahmad, K. Shah, T. Abdeljawad, Iterative analysis of nonlinear BBM equations under nonsingular fractional order derivative, *Advances in Mathematical Physics*, **2020** (2020), 3131856. http://doi.org/10.1155/2020/3131856
3. I. Podlubny, *Fractional Differential Equations*, San Diego: Academic Press, 1999.
4. A. A. Kilbas, H. M. Srivastava, J. J. Trujillo, *Theory and Applications of Fractional Differential Equations*, Amsterdam: Elsevier, 2006.
5. R. Hilfer, *Applications of Fractional Calculus in Physics*, Singapore: World Scientific, 2000.

6. R. L. Magin, *Fractional Calculus in Bioengineering*, New York: Begell House, 2006.
7. H. Alrabaiah, I. Ahmad, K. Shah, I. Mahariq, G. U. Rahman, Analytical solution of non-linear fractional order Swift-Hohenberg equations, *Ain Shams Eng. J.*, **12** (2021), 3099–3107. http://doi.org/10.1016/j.asej.2020.11.019
8. V. E. Tarasov, *Fractional Dynamics: Applications of Fractional Calculus to Dynamics of Particles, Fields and Media*, Berlin: Springer, 2011.
9. F. Mainardi, Fractional relaxation-oscillation and fractional diffusion-wave phenomena, *Chaos, Soliton. Fract.*, **7** (1996), 1461–1477. http://doi.org/10.1016/0960-0779(95)00125-5
10. D. Baleanu, K. Diethelm, E. Scalas, J. J. Trujillo, *Fractional Calculus: Models and Numerical Methods*, Singapore: World Scientific, 2012.
11. A. Bekir, Ö. Güner, Ö. Ünsal, The first integral method for exact solutions of nonlinear fractional differential equations, *J. Comput. Nonlinear Dyn.* **10** (2015), 021020-5. http://doi.org/10.1115/1.4028065
12. E. A. Az-Zo'bi, Q. M. M. Alomari, K. Afef, M. Inc, Dynamics of generalized time-fractional viscous-capillarity compressible fluid model, *Opt. Quant. Electron.*, **56** (2024), 629. http://doi.org/10.1007/s11082-023-06233-2
13. Y. Zhou, *Basic theory of fractional differential equations*, Singapore: World scientific, 2023.
14. E. Hussain, Z. Li, S. A. A Shah, E. A. Az-Zo'bi, M. Hussien, Dynamics study of stability analysis, sensitivity insights and precise soliton solutions of the nonlinear (STO)-Burger equation, *Opt. Quant. Electron.*, **55** (2023), 1274. http://doi.org/10.1007/s11082-023-05588-w
15. M. A. Al Zubi, K. Afef, E. A. Az-Zo'bi, Assorted spatial optical dynamics of a generalized fractional quadruple nematic liquid crystal system in non-local media, *Symmetry*, **16** (2024), 778. http://doi.org/10.3390/sym16060778
16. J. H. He, Homotopy perturbation technique, *Comput. Math. Appl.*, **57** (1999), 410–412. http://doi.org/10.1016/S0045-7825(99)00018-3
17. R. Khalil, M. Al Horani, A. Yousef, M. A. Sababheh, New definition of fractional derivative, *J. Comput. Appl. Math.*, **264** (2014), 65–70. http://doi.org/10.1016/j.cam.2014.01.002
18. H. U.Rehman, I. Iqbal, S. S. Aiadi, N. Mlaiki, M. S. Saleem, Soliton solutions of Klein-Fock-Gordon equation using Sardar subequation method, *Mathematics,* **10** (2022), 3377.
19. H. U. Rehman, I. Iqbal, M. Mirzazadeh, S. Haque, N. Mlaiki, W. Shatanawi, Dynamical behavior of perturbed Gerdjikov-Ivanov equation through different techniques, *Bound. Value Prob.*, **2023** (2023), 105. http://doi.org/10.1186/s13661-023-01792-5
20. C. S. Gardner, J. M. Greene, M. D. Kruskal, R. M. Miura, Method for solving the Korteweg-deVries equation, *Phys. Rev. Lett.*, **19** (1967), 1095. http://doi.org/10.1103/PhysRevLett.19.1095
21. T. B. Benjamin, J. L. Bona, J. J. Mahony, Model equations for long waves in nonlinear dispersive systems, *Philos. T. R. Soc. A*, **272** (1972), 47–78. http://doi.org/10.1098/rsta.1972.0032
22. C. Li, Linearized difference schemes for a BBM equation with a fractional nonlocal viscous term, *Appl. Math. Comput.*, **311** (2017), 240–250. http://doi.org/10.1016/j.amc.2017.05.022

23. A. Saadatmandi, M. A. Dehghan, A new operational matrix for solving fractional-order differential equations, *Comput. Math. Appl.*, **59** (2010), 1326–1336. http://doi.org/10.1016/j.camwa.2009.07.006

24. E. Hussain, S. A. A. Shah, A. Bariq, Z. Li, M. R. Ahmad, A. E. Ragab, et al., Solitonic solutions and stability analysis of Benjamin Bona Mahony Burger equation using two versatile techniques, *Sci. Rep.*, **14** (2024), 13520. http://doi.org/10.1038/s41598-024-60732-0

25. M. Kamran, M. Abbas, A. Majeed, H. Emadifar, T. Nazir, Numerical simulation of time fractional BBM-Burger equation using cubic B-spline functions, *J. Function Spaces*, **2022** (2022), 2119416. http://doi.org/10.1155/2022/2119416

26. A. M. Wazwaz, A reliable modification of Adomian decomposition method, *Appl. Math. Comput.*, **102** (1999), 77–86. http://doi.org/10.1016/S0096-3003(98)10024-3

27. Z. Yan, J. Li, S. Barak, S. Haque, N. Mlaiki, Delving into quasi-periodic type optical solitons in fully nonlinear complex structured perturbed Gerdjikov-Ivanov equation, *Sci. Rep.*, **15** (2025), 8818. http://doi.org/10.1038/s41598-025-91978-x

28. S. Liao, *Beyond Perturbation: Introduction to the Homotopy Analysis Method*, New York: Chapman & Hall/CRC, 2003.

29. A. R. Appadu, A. S. Kelil, N. W. Nyingong, Solving a fractional diffusion PDE using some standard and nonstandard finite difference methods with conformable and Caputo operators, *Front. Appl. Math. Stat.*, **10** (2024), 1358485 . http://doi.org/10.3389/fams.2024.1358485

30. Y. Zou, Y. Cui, Uniqueness criteria for initial value problem of conformable fractional differential equation, *Electron. Res. Arch.*, **31** (2023), 4077–4087. http://doi.org/10.3934/era.2023207

31. T. Abdeljawad, On conformable fractional calculus, *J. Comput. Appl. Math.*, **279** (2015), 57–66. http://doi.org/10.1016/j.cam.2014.10.016

32. H. Khan, J. Alzabut, D. Baleanu, G. Alobaidi, M. U. Rehman, Existence of solutions and a numerical scheme for a generalized hybrid class of n-coupled modified ABC-fractional differential equations with an application, *AIMS Mathematics*, **8** (2023), 6609–6625. http://doi.org/10.3934/math.2023334

33. E. A. Az-Zo'bi, R. Shah, H. A. Alyousef, C. G. L. Tiofack, S. A. El-Tantawy, On the feed-forward neural network for analyzing pantograph equations, *AIP Adv.*, **14** (2024), 025042.http://doi.org/10.1063/5.0195270

34. A. R. Appadu, G. N. de Waal, C. J. Pretorius, Nonstandard finite difference methods for a convective predator-prey pursuit and evasion model, *J. Differ. Equ. Appl.*, **30** (2024), 1808–1841. http://doi.org/10.1080/10236198.2024.2361115

35. R. E. Mickens, *Applications of Nonstandard Finite Difference Schemes*, Singapore: World Scientific, 2000.

36. M. Raissi, P. Perdikaris, G. E. Karniadakis, Physics-informed neural networks: A deep learning framework for solving forward and inverse problems involving nonlinear partial differential equations, *J. Comput. Phys.*, **378** (2019), 686–707. http://doi.org/10.1016/j.jcp.2018.10.045

37. L. Lu, P. Jin, G. Pang, Z. Zhang, G. E. Karniadakis, Learning nonlinear operators via DeepONet based on the universal approximation theorem of operators, *Nat. Mach. Intell.*, **3** (2021), 218–229. http://doi.org/10.1038/s42256-021-00302-5

38. H. S. Alruhaili, A. S. Hussain, A. Ajlouni, F. Türk, E. A. Az-Zo'bi, M. Tashtoush, Solving Time-Fractional Nonlinear Variable-Order Delay PDEs Using Feedforward Neural Networks, *Iraqi J. Comput. Sci. Math.*, **6** (2025), 12. http://doi.org/10.52866/2788-7421.1284

AIMS Press